QUARTERLY OF APPLIED MATHEMATICS

VOLUME LII JUNE · 1994 NUMBER 2

JUNE 1994, PAGES 201–228

THE ENERGY RELEASE RATE FOR TRANSIENT DYNAMIC MODE I CRACK PROPAGATION IN A GENERAL LINEARLY VISCOELASTIC BODY

BY

J. M. HERRMANN AND J. R. WALTON

Texas A & M University, College Station, Texas

Abstract. A mathematical model of a semi-infinite mode I crack that suddenly begins to propagate at constant speed is constructed for a general linear viscoelastic body. Expressions for the Laplace transform of the stress, displacement, and stress intensity factor are derived for general loadings. A Barenblatt type process zone is incorporated into the model and used to determine the total energy flux into the crack tip. This energy release rate, $G(t)$, is constructed for two specific loadings: one following the advancing crack tip, the second remaining fixed as the crack tip advances. In each case $G(t)$ is analyzed by asymptotic and numerical methods to determine its qualitative form and, in particular, its rate of decay to its steady-state value. The effect of such simplifying assumptions as quasi-static propagation or an elastic material is also illustrated. The second loading is intended as an idealized model of the dynamic fracture experiments of Ravi-Chandar and Knauss [13–16].

1. Introduction. The analytical study of dynamically propagating cracks in linearly viscoelastic material was begun by the Willis [26] study which constructed the dynamic steady state stress intensity factor (SIF) for a propagating semi-infinite, mode III, (antiplane shear) crack in an infinite viscoelastic body modelled as a standard linear solid. Extensions and generalizations of this work have been accomplished by several researchers, e.g., Atkinson and List [5], Atkinson and Coleman [4], Atkinson [3], Atkinson and Popelar [6], Popelar and Atkinson [12], Walton [20–24], Schovanec and Walton [17–19], and Herrmann and Schovanec [9]. A synopsis of this previous work can be found in Herrmann and Walton [10].

Herrmann and Walton [10] derived analytical expressions for the stresses, displacements, and stress intensity factor for a semi-infinite mode III crack, initially at rest, which begins to propagate at a constant speed under the action of suddenly applied loads on the crack faces. The loads are completely general and can be time varying. These were the first transient dynamic results for a very general class of viscoelastic

Received July 26, 1991.

1991 *Mathematics Subject Classification.* Primary 73M25; Secondary 73F15, 73V35.

Each author gratefully acknowledges the support for this research provided by the Air Force Office of Scientific Research and the National Science Foundation through the NSF Grant No. DMS-8903672.

material models which includes both the power law and standard linear solid viscoelastic models. Herrmann and Walton [10] also presented closed form expressions for the Laplace transform of an energy release rate. A Barenblatt type process zone behind the crack tip was incorporated into the model, and the energy flux into this damage zone per unit crack advance was derived for time varying loadings which follow the advancing crack tip and which have a particular spatial form. This energy release rate was found to be the product of the response stress in the process zone and an energy integral. An expression for the Laplace transform of each of these functions was derived and the mathematical behavior of the energy release rate was studied through asymptotic methods and through the consideration of special cases such as quasi-static crack propagation or an elastic material model. Herrmann and Walton [11] showed that these formulas could be generalized to the complex plane and thus numerical Laplace inversion along a Bromwich path was valid. The numerous graphs displayed in Herrmann and Walton [11] showed the effect on the energy release rate of varying the different nondimensional parameters identified in these formulae.

The purpose of this paper is to extend these models to the more applicable and difficult case of transient dynamic mode I crack propagation. In particular, it is intended thereby to model (at least qualitatively) the fundamental dynamic fracture experiments described in Ravi-Chandar and Knauss [13–16]. In these experiments, a large plate with a starter crack had a fixed part of its crack faces loaded by a copper strip which provided an opening mode pressure when a capacitor-inductor circuit was discharged through the strip. The size of the plate was chosen large enough so that reflected waves did not interact with the crack tip for the duration of the experiment thus simulating an infinite specimen geometry in their experiments. It was discovered from examining the caustics resulting from the crack tip stress field in their birefringent material that the crack tip advanced at a constant speed even though the stress intensity factor was varying. Furthermore, the initial acceleration phase of the crack tip could not be observed since it occurred in a time period of less than the 5 μ sec that the experiments high speed photography could resolve. Similarly, in their studies of crack arrest no deceleration was observed since the arrest also occurred in a time period of less than 5μ sec. Ravi-Chandar and Knauss concluded from a series of experiments which varied the duration of the loading on the crack faces that "the question of whether a crack will initiate under some applied loading into unstable growth depends not only on the amplitude of the loading, but also on the complete history of load application." Their observations support the value of studying the constant crack speed model considered here.

Our mathematical model assumes a general viscoelastic material whose current state of stress depends on the complete history of the strain of the material through Riemann-Stieltjes convolutions of the shear modulus μ and Lame modulus λ with the strain. For a semi-infinite mode I crack that begins to propagate at a constant speed less than the glassy shear wave speed, the authors derive expressions for the Laplace transform of the stresses, the displacements, and the stress intensity factor. Furthermore, a Barenblatt type process zone is incorporated behind the crack tip,

and an expression for the energy flux into this damage zone is determined. This energy release rate is derived for two different loading schemes; the first assumes the load on the crack faces follows the advancing crack tip as in the previous studies of Herrmann and Walton (1989, 1991), and the second loading assumes that the crack face tractions remain fixed as the crack tip advances. The energy release rate in each case is found to be the product of the response stress in the damage zone and an energy integral. The Laplace transforms of each of these functions are determined for complex values of the Laplace variable so that numerical Laplace inversion of these expressions is valid. The behavior of these expressions is investigated by asymptotic as well as numerical means. Moreover, the effect of such simplifying assumptions as quasi-static propagation or an elastic material model is also examined. In particular, it will be seen that the first loading scheme has the energy release rate quickly and monotonically rise to its steady state value while the second loading scheme has a quick monotonic increase to a peak value and then a monotonic decrease to zero. If it is assumed that a minimum energy input to the crack tip is necessary for continued crack propagation, then this behavior of the energy release rate under the second loading scheme, which reflects the essential features of that occurring in the experiments of Ravi-Chandar and Knauss, suggests that the crack should slow or arrest if the crack could be observed for a long enough time.

2. Problem formulation and reduction to a Riemann-Hilbert problem. The problem to be considered is that of a semi-infinite mode I crack that begins to propagate at a constant speed V in an infinite isotropic, homogeneous, linearly viscoelastic body due to the sudden application of crack face tractions that travel with the crack. The crack is assumed to initially lie along the negative x_1-axis and to begin to propagate with a constant speed V at time $t = 0$. The deformation is assumed to be plane strain and symmetric about the plane of the crack. The equations of motion are

$$\rho \ddot{u}_i = \sigma_{ij,j} \quad \text{for } x_2 > 0 \text{ and } i = 1, 2 \tag{2.1}$$

with initial conditions

$$u_i(x_1, x_2, 0) = 0, \qquad \dot{u}_i(x_1, x_2, 0) = 0, \tag{2.2}$$

and boundary conditions

$$\begin{aligned} &\sigma_{12}(x_1, 0, t) = 0 \quad \text{for } -\infty < x_1 < \infty, \\ &\sigma_{22}(x_1, 0, t) = L_e \Lambda_e \left(\frac{x_1 - Vt}{a_e}, t \right) \quad \text{for } x_1 < Vt, \\ &u_2(x_1, 0, t) = 0 \quad \text{for } x_1 > Vt, \\ &\sigma_{ij}(x_1, x_2, t) \to 0 \quad \text{as } x_1^2 + x_2^2 \to \infty, \end{aligned} \tag{2.3}$$

where u_i and σ_{ij} are the displacement and stress tensor components, ρ is the mass density, and $L_e \Lambda_e((x_1 - Vt)/a_e, t)$ denotes the crack face normal traction. $\Lambda_e(\,)$ is dimensionless while a_e and L_e have the dimensions of length and stress, respectively. Also, while the crack speed is assumed to be constant, the driving load is allowed to be time varying. The constitutive relations are given by

$$\sigma_{ij} = 2\mu * d\varepsilon_{ij} + \delta_{ij} \lambda * d\varepsilon_{kk}, \tag{2.4}$$

in which ε_{ij} are the strain tensor components, μ and λ are positive, decreasing functions of $t > 0$, and $\mu * d\varepsilon$ denotes the Riemann-Stieltjes convolution

$$\mu * d\varepsilon = \int_{-\infty}^{t} \mu(t-\tau)d\varepsilon(\tau).$$

We shall adopt the moving coordinate system (x, y, t) given by $x = x_1 - Vt$, $y = x_2$ and define $u(x, y, t) = u(x_1 - Vt, x_2, t) = u_1(x_1, x_2, t)$ and $v(x, y, t) = u_2(x_1, x_2, t)$. In the moving coordinate system, (2.1) becomes for $y > 0$

$$\begin{aligned}
\rho\left[\frac{\partial}{\partial t} - V\frac{\partial}{\partial x}\right]^2 u(x, y, t) &= \frac{\partial^2}{\partial x^2}[(2\mu+\lambda) * du] + \frac{\partial^2}{\partial y^2}[u * du] \\
&\quad + \frac{\partial^2}{\partial x \partial y}[(\mu+\lambda) * dv], \\
\rho\left[\frac{\partial}{\partial t} - V\frac{\partial}{\partial x}\right]^2 u(x, y, t) &= \frac{\partial^2}{\partial x^2}[(2\mu+\lambda) * du] + \frac{\partial^2}{\partial y^2}[u * dv] \\
&\quad + \frac{\partial^2}{\partial x \partial y}[(\mu+\lambda) * du].
\end{aligned} \tag{2.5}$$

A Helmholtz decomposition shall now be introduced. The potentials θ and φ are defined as the solutions to

$$\begin{aligned}
\rho\left[\frac{\partial}{\partial t} - V\frac{\partial}{\partial x}\right]^2 \theta(x, y, t) &= \Delta[(2\mu+\lambda) * d\theta], \\
\rho\left[\frac{\partial}{\partial t} - V\frac{\partial}{\partial x}\right]^2 \varphi(x, y, t) &= \Delta[\mu * d\varphi],
\end{aligned} \tag{2.6}$$

where $\Delta = \partial^2/\partial x^2 + \partial^2/\partial y^2$. Equation (2.5) will then be satisfied by writing

$$u(x, y, t) = \frac{\partial}{\partial x}\theta(x, y, t) + \frac{\partial}{\partial y}\varphi(x, y, t)$$

and

$$v(x, y, t) = \frac{\partial}{\partial y}\theta(x, y, t) - \frac{\partial}{\partial x}\varphi(x, y, t).$$

Application of the Fourier transform, $\hat{f}(p, y, t) = \int_{-\infty}^{\infty} e^{ipx} f(x, y, t)\,dx$, to (2.6) followed by the Laplace transform $\overline{g}(p, y, s) = \int_0^{\infty} g(p, y, \tau)e^{-s\tau}\,d\tau$, produces the ordinary differential equations in y,

$$\begin{aligned}
\rho[s + iVp]^2\hat{\bar{\theta}}(p, y, s) &= \left[\frac{\partial^2}{\partial y^2} - p^2\right][(2\tilde{\mu}+\tilde{\lambda})(s + iVp)\hat{\bar{\theta}}(p, y, s)], \\
\rho[s + iVp]^2\hat{\bar{\varphi}}(p, y, s) &= \left[\frac{\partial^2}{\partial y^2} - p^2\right][(\tilde{\mu}(s + iVp)\hat{\bar{\varphi}}(p, y, s)],
\end{aligned} \tag{2.7}$$

where $\tilde{\mu}(s)$ denotes the Carson transform $\tilde{\mu}(s) = \mu(0) + \int_0^{\infty} e^{-s\tau}\,d\mu(\tau)$. The solutions of (2.7) are

$$\hat{\bar{\theta}}(p, y, s) = A(p, s)e^{-\beta_1(p,s)y} \quad \text{and} \quad \hat{\bar{\varphi}}(p, y, s) = B(p, s)e^{-\beta_2(p,s)y}, \tag{2.8}$$

where

$$\beta_1(p, s) = \left[p^2 + \frac{\rho(s + iVp)^2}{(2\tilde{\mu} + \tilde{\lambda})(s + iVp)}\right]^{1/2} \quad \text{and} \quad \beta_2(p, s) = \left[p^2 + \frac{\rho(s + iVp)^2}{\tilde{\mu}(s + iVp)}\right]^{1/2}$$

must be chosen to have positive real parts to ensure that $\hat{\bar{\theta}}(p, y, s)$ and $\hat{\bar{\varphi}}(p, y, s) \to 0$ as $y \to \infty$.

In a similar manner the Fourier and Laplace transforms are applied to the boundary condition $\sigma_{12}(x_1, 0, t) = 0$, $-\infty < x_1 < \infty$, with the result that $A(p, s)$ and $B(p, s)$ must satisfy

$$B(p, s) = \frac{-2ip\beta_1(p, s)}{p^2 + \beta_2(p, s)^2} A(p, s). \tag{2.9}$$

Similarly, taking the Fourier and Laplace transforms of $\sigma_{22}(x_1, 0, t) = \sigma_{yy}(x, 0, t)$ one has that

$$\hat{\bar{\sigma}}_{yy}(p, 0, s) = (2\tilde{\mu} + \tilde{\lambda})(s + iVp)\frac{\partial}{\partial y}\hat{\bar{v}}(p, 0, s) + (-ip)\tilde{\lambda}(s + iVp)\hat{\bar{u}}(p, 0, s). \tag{2.10}$$

From the Helmholtz potentials, it can be seen that

$$\hat{\bar{u}}(p, 0, s) = \left[-ip\hat{\bar{\theta}}(p, 0, s) + \frac{\partial}{\partial y}\hat{\bar{\varphi}}(p, 0, s)\right] = -ipA - \beta_2 B,$$

$$\hat{\bar{v}}(p, 0, s) = -\beta_1 A + ipB,$$

and $\frac{\partial}{\partial y}\hat{\bar{v}}(p, 0, s) = \beta_1^2 A - ip\beta_2 B$. Thus (2.10) may be written as

$$\hat{\bar{\sigma}}^+_{yy}(p, 0, s) + \hat{\bar{\sigma}}^-_{yy}(p, 0, s) = T(p)\hat{\bar{v}}(p, 0, s) \tag{2.11}$$

where $\hat{f}^+(p)$ and $\hat{f}^-(p)$ denote

$$\hat{f}^+(p) = \int_0^\infty e^{ipx} f(x)\, dx \quad \text{and} \quad \hat{f}^-(p) = \int_{-\infty}^0 e^{ipx} f(x)\, dx,$$

and

$$T(p) = \frac{2\tilde{\mu}(s + iVp)[\beta_1^2(p^2 + \beta_2^2) - 2p^2\beta_1\beta_2] + \tilde{\lambda}(s + iVp)(\beta_1^2 - p^2)(p^2 + \beta_2^2)}{\beta_1(p^2 - \beta_2^2)}.$$

Since $v(x, 0, t) = 0$ for $x > 0$ then $\hat{\bar{v}}(p, 0, s) = \hat{\bar{v}}^-(p, 0, s)$. It is assumed a priori (and is easily verified a posteriori) that $\hat{\bar{v}}^-(p, 0, s)$ and $\hat{\bar{\sigma}}^+_{yy}(p, 0, s)$ have analytic extensions $\hat{\bar{v}}^-(z, 0, s)$ and $\hat{\bar{\sigma}}^+_{yy}(z, 0, s)$ for $\mathrm{Im}(z) < 0$ and $\mathrm{Im}(z) > 0$, respectively, which vanish as $|z| \to \infty$. Thus the boundary condition (2.11) may be reformulated into the Riemann-Hilbert problem: find $F^+(z)$ analytic for $\mathrm{Im}(z) > 0$ and $F^-(z)$ analytic for $\mathrm{Im}(z) < 0$ such that $\lim_{\mathrm{Im}(z)\to+\infty} F^+(z) = \lim_{\mathrm{Im}(z)\to-\infty} F^-(z) = 0$ and on $\mathrm{Im}(z) = 0$,

$$F^+(p) = T(p)F^-(p) - g(p) \quad \text{for } p \in (-\infty, \infty) \tag{2.12}$$

where $F^+(z) = \hat{\bar{\sigma}}^+_{yy}(z, 0, s)$, $F^-(z) = \hat{\bar{v}}^-(z, 0, s)$, and

$$g(p) = \hat{\bar{\sigma}}^-_{yy}(p, 0, s) = L_e a_e \hat{\bar{\Lambda}}_e(a_e p, s).$$

For convenience, explicit reference to the s dependence of $T(p)$, $g(p)$, and $F^{\pm}(z)$ is being suppressed.

So as not to introduce more mathematical complications, Poisson's ratio is assumed to be constant. From this assumption, it follows that $\lambda = \frac{2\nu}{1-2\nu}\mu$. Furthermore $\beta_1(p)$ and $T(p)$ may be simplified with

$$\beta_1(p, s) = \left[p^2 + \frac{k_1 \rho(s + iVp)^2}{\tilde{\mu}(s + iVp)}\right]^{1/2} \tag{2.13}$$

where $k_1 = \frac{1-2\nu}{2(1-\nu)}$, and

$$T(p) = \frac{[\tilde{\mu}(s + iVp)]^2}{(s + iVp)^2 \rho \beta_1}[4p^2\beta_1\beta_2 - (p^2 + \beta_2^2)^2]. \tag{2.14}$$

It is easily seen that the physically relevant solution of (2.12) is given by

$$F^{\pm}(z) = X^{\pm}(z)\frac{1}{2\pi i}\int_{-\infty}^{\infty} \frac{-g(\tau)}{X^{+}(\tau)}\frac{d\tau}{\tau - z}, \tag{2.15}$$

where $X^{\pm}(z)$ solves the homogeneous Riemann-Hilbert problem

$$X^{+}(p) = T(p)X^{-}(p) \quad \text{for } p \in (-\infty, \infty). \tag{2.16}$$

To solve (2.16), it is convenient to factor $T(p)$ into the product $T(p) = T_1(p)T_2(p)T_3(p)$ in which

$$T_1(p) = \frac{[\tilde{\mu}(s + iVp)]^2}{\rho(s + iVp)^2}, \quad T_2(p) = \beta_1^{-1}, \quad T_3(p) = 4p^2\beta_1\beta_2 - (p^2 + \beta_2^2)^2.$$

$X^{\pm}(z)$ may now be constructed as the product $X^{\pm}(z) = X_1^{\pm}(z)X_2^{\pm}(z)X_3^{\pm}(z)$ with each $X_i^{\pm}(z)$ satisfying the Riemann-Hilbert problem $X_i^{+}(p) = T_i(p)X_i^{-}(p)$.

For the subsequent analysis the shear modulus will be assumed to be positive, continuously differentiable, nonincreasing, convex and such that $\mu(\infty) = \lim_{t\to\infty} \mu(t) > 0$. Convexity is sufficient but certainly not necessary to insure the validity of the following calculations and though theoretically overly restrictive, it holds for most of the customary models such as a standard linear solid or a power-law material. The analysis is also valid under the more general assumption that $\overline{\mu}(is)$ has a negative, semidefinite imaginary part which for constant Poisson's ratio guarantees that the second law of thermodynamics holds. This condition is satisfied by an Achenbach-Chao material, for example, for which $\mu(t)$ is neither decreasing nor convex. Moreover, it is worth noting that no explicit time decay rate for the shear modulus needs to be specified for the results to be valid.

In the following analysis it shall be necessary to allow the fixed value of s in (2.16) to be complex with positive real part so that numerical Laplace inversion along a Bromwich path can be done. First, to determine $X_1^{\pm}(z)$, it easily follows from the fact that $\mu(t) = 0$ for $t < 0$ that $[\tilde{\mu}(s + iVz)]^{-1}$ is analytic for $\mathrm{Im}(z) < 0$. Furthermore $(s + iVz)^2$ is also analytic for $\mathrm{Im}(z) < 0$ and therefore one may choose

$$X_1^{+}(z) = 1 \quad \text{and} \quad X_1^{-}(z) = \rho(s + iVz)^2[\tilde{\mu}(s + iVz)]^{-2}. \tag{2.17}$$

Before determining $X_2^{\pm}(z)$ and $X_3^{\pm}(z)$, it is necessary to investigate the properties of

$$F(p, s, k) = \frac{p^2}{(p - is/V)^2} - \frac{k\rho V^2}{\tilde{\mu}(s + iVp)}$$

where s and k are fixed and such that $\mathrm{Re}(s) > 0$ and $k > 0$. It can be easily shown that $\mathrm{Im}[F(p, s, k)] < 0$ for $p < -\mathrm{Im}(s)/V$ and $\mathrm{Im}[F(p, s, k)] > 0$ for $p > -\mathrm{Im}(s)/V$. Furthermore, $F(-\mathrm{Im}(s)/V, s, k) < 0$ and

$$F(\pm\infty, s, k) = 1 - \frac{k\rho V^2}{\mu(0)} > 0 \quad \text{for } 0 < V < \left[\frac{\mu(0)}{\rho k}\right]^{1/2}.$$

Thus, the closed curve defined by $F(p, s, k)$ as $-\infty < p < \infty$ has a winding number of one about the origin and therefore, by the argument principle, there exists in the lower half-plane, $\mathrm{Im}(z) < 0$, a unique root of order one, $z_* = z_*(s, k)$, of $F(z_*, s, k) = 0$.

We shall now write $\beta_1(p, s) = \mathrm{sgn}(p + \mathrm{Im}(s)/V)(p - is/V)F(p, s, k_1)^{1/2}$. Note that $k_1 = \frac{1-2\nu}{2(1-\nu)}$ is such that $0 < k_1 < \frac{1}{2}$ if $0 < \nu < \frac{1}{2}$. We shall choose a branch cut for $F(p, s, k_1)^{1/2}$ such that $F(p, s, k_1)^{1/2}$ is continuous except for a jump discontinuity at $p = -\mathrm{Im}(s)/V$ where $F(p, s, k) \to \pm i|F(-\mathrm{Im}(s)/V, s, k)|^{1/2}$ as $p \to -\mathrm{Im}(s)/V\pm$. Moreover, $\mathrm{Im}[\mathrm{sgn}(p + \mathrm{Im}(s)/V)(p - is/V)] > 0$ for $p < -\mathrm{Im}(s)/V$ and $\mathrm{Im}[\mathrm{sgn}(p + \mathrm{Im}(s)/V)(p - is/V)] < 0$ for $p > -\mathrm{Im}(s)/V$ with $\mathrm{sgn}(p + \mathrm{Im}(s)/V)(p - is/V) \to \mp i\,\mathrm{Re}[s]/V$ as $p \to -\mathrm{Im}(s)/V\pm$. Thus, this form of β_1 insures that $\mathrm{Re}[\beta_1(p, s)] > 0$.

We shall write $T_2(p) = \beta_1(p, s)^{-1} = T_{21}(p)T_{22}(p)$ where

$$T_{21}(p) = \frac{\mathrm{sgn}(p + \mathrm{Im}(s)/V)}{p - is/V} \quad \text{and } T_{22}(p) = F(p, s, k_1)^{-1/2}.$$

It can be shown that

$$X_{21}^{+}(z) = \omega^{+}(z + \mathrm{Im}(s)/V) \quad \text{and} \quad X_{21}^{-}(z) = (z - is/V)\omega^{-}(z + \mathrm{Im}(s)/V)$$

satisfies $X_{21}^{+}(p) = T_{21}(p)X_{21}^{-}(p)$ where $\omega^{+}(z)$ denotes $z^{1/2}$ with branch cut along the negative imaginary axis and $\omega^{-}(z)$ denotes $z^{1/2}$ with branch cut along the positive imaginary axis. $X_{22}^{\pm}(z)$ such that $X_{22}^{+}(p) = T_{22}(p)X_{22}^{-}(p)$ can be constructed as $X_{22}^{\pm}(z) = \exp(\Gamma^{\pm}(z))$ where

$$\Gamma^{\pm}(z) = \frac{1}{2\pi i}\int_{-\infty}^{\infty} \frac{\log(F(\tau, s, k_1)^{-1/2})}{\tau - z}\, d\tau.$$

The branch cut for $F(z, s, k_1)^{1/2}$ shall be chosen as the line segment L_1 connecting $-\mathrm{Im}(s)/V$ and the unique zero $z_1 \equiv z_*(s, k_1)$ of $F(z, s, k_1)$ for $\mathrm{Im}[z] \leq 0$. Therefore $F(p, s, k_1)^{-1/2}$ is analytic for z in the lower half-plane except along L_1 and the integral for $\Gamma^{\pm}(z)$ can be done by residues. It is found that

$$X_{22}^{+}(z) = \left(\frac{z + \mathrm{Im}(s)/V}{z - z_1}\right)^{1/2} \quad \text{and} \quad X_{22}^{-}(z) = \left(\frac{z + \mathrm{Im}(s)/V}{z - z_1}\right)^{1/2} F(z, s, k_1)^{1/2},$$

where the branch cuts are along L_1. Since $X_2^{\pm}(z) = X_{21}^{\pm}(z)X_{22}^{\pm}(z)$ then

$$X_2^{+}(z) = \omega^{+}(z + \mathrm{Im}(s)/V)\left(\frac{z + \mathrm{Im}(s)/V}{z - z_1}\right)^{1/2},$$
$$X_2^{-}(z) = (z - is/V)\omega^{-}(z + \mathrm{Im}(s)/V)\left(\frac{z + \mathrm{Im}(s)/V}{z - z_1}\right)^{1/2} F(z, s, k_1)^{1/2}. \tag{2.18}$$

Finally, we need to determine $X_3^{\pm}(z)$ such that $X_3^{+}(p) = T_3(p)X_3^{-}(p)$ where $T_3(p) = 4p^2\beta_1\beta_2(p^2 + \beta_2^2)^2$. To aid in this, we shall write

$$T_3(p) = T_{31}(p)T_{32}(p) \quad \text{where } T_{31}(p) = 4(p - is/V)^4$$

and

$$T_{32}(p) = \frac{p^2}{(p - is/V)^2} F(p, s, k_1)^{1/2} F(p, s, 1)^{1/2} - F(p, s, 1/2)^2.$$

Note that each β_j has been written as

$$\beta_j(p, s) = \mathrm{sgn}(p + \mathrm{Im}(s)/V)(p - is/V)F(p, s, k_j)^{1/2}$$

where $k_2 \equiv 1$. In each case this guarantees that $\mathrm{Re}[\beta_j(p, s)] > 0$. Choosing $X_{31}^{+}(z) = 4$ and $X_{31}^{-}(z) = (z - is/V)^{-4}$, we see that $X_{31}^{+}(p) = T_{31}(p)X_{31}^{-}(p)$.

We shall now determine $X_{32}^{\pm}(z)$ in a manner similar to $X_{22}^{\pm}(z)$. First, we shall extend $T_{32}(p)$ to the lower half-plane by choosing the branch cut of $F(z, s, k_1)^{1/2}$ from $-\mathrm{Im}[s]/V$ to z_1 along L_1 as discussed above and choosing the branch cut for $F(z, s, 1)^{1/2}$ from $-\mathrm{Im}[s]/V$ to $z_2 \equiv z_*(s, 1)$ along $L_1 \cup L_2$ where L_2 is the line segment from z_1 to z_2. It may be seen that $T_{32}(p)$ for $-\infty \le p \le \infty$ defines a closed curve since

$$T_{32}(\infty) = [1 - k_1\rho V^2/\mu(0)]^{1/2}[1 - \rho V^2/\mu(0)]^{1/2} - [1 - \tfrac{1}{2}\rho V^2/\mu(0)]^2.$$

The function

$$R(x) = [1 - k_1 x]^{1/2}[1 - x]^{1/2} - [1 - x/2]^2 \tag{2.19}$$

can be shown by the argument principle to have exactly two zeros. Note that $R(0) = 0$, $R(1) < 0$, and $R'(0) > 0$; thus the second zero of $R(x)$, r_0, is such that $0 < r_0 < 1$. Furthermore, $R(x)$ is positive for $0 < x < r_0$ and negative for $-\infty < x < 0$. Thus for $V < [r_0\mu(0)/\rho]^{1/2}$, $T_{32}(\infty) > 0$. Moreover,

$$T_{32}(-\mathrm{Im}[s]/V) = \left(\frac{\mathrm{Im}[s]}{\mathrm{Re}[s]}\right)^4 R\left(-\left(\frac{\mathrm{Im}[s]}{\mathrm{Re}[s]}\right)^2 \frac{\rho V^2}{\tilde{\mu}(\mathrm{Re}[s])}\right) < 0.$$

By examining the curve defined for $T_{32}(p)$ for $-\infty \le p \le \infty$ it can be seen that the winding number of the curve about the origin is one and thus $T_{32}(z)$ has a unique zero in the lower half-plane which we will denote z_3. Thus $\log(T_{32}(z))$ can be defined by choosing a branch cut along $L_1 \cup L_2 \cup L_3$ where L_3 is the line segment

from z_2 to z_3 off of which $\log(T_{32}(z))$ is analytic for z in the lower half-plane. $\Gamma^{\pm}(z)$ can now be determined by residues as before with the result that

$$X_{32}^{+}(z) = \left(\frac{z - z_1}{z + \mathrm{Im}[s]/V}\right)\left(\frac{z - z_3}{z - z_2}\right) e^{I_{32}(z)}$$

and

$$X_{32}^{-}(z) = \left(\frac{z - z_1}{z + \mathrm{Im}[s]/V}\right)\left(\frac{z - z_3}{z - z_2}\right) \frac{e^{I_{32}(z)}}{T_{32}(z)}$$

where

$$I_{32} \equiv \frac{1}{2\pi i}\int_{L_2} \frac{\log(T_{32}(\tau^{+})) - \log(T_{32}(\tau^{-}))}{\tau - z}\, d\tau .$$

Thus

$$\begin{aligned} X_3^{+}(z) &= 4\left(\frac{z - z_1}{z + \mathrm{Im}[s]/V}\right)\left(\frac{z - z_3}{z - z_2}\right) e^{I_{32}(z)}, \\ X_3^{-}(z) &= (z - is/V)^{-4}\left(\frac{z - z_1}{z + \mathrm{Im}[s]/V}\right)\left(\frac{z - z_3}{z - z_2}\right)\frac{e^{I_{32}(z)}}{T_{32}(z)}. \end{aligned} \tag{2.20}$$

Combining (2.17), (2.18), and (2.20), $X^{\pm}(z)$ is seen to be

$$\begin{aligned} X^{+}(z) &= 4\omega^{+}(z + \mathrm{Im}(s)/V)\left(\frac{z + \mathrm{Im}(s)/V}{z - z_1}\right)^{1/2}\left(\frac{z - z_1}{z + \mathrm{Im}[s]/V}\right)\left(\frac{z - z_3}{z - z_2}\right) e^{I_{32}(z)}, \\ X^{-}(z) &= \frac{-\rho V^2}{\tilde{\mu}(s + iVz)^2}\frac{1}{z - is/V}\omega^{-}(z + \mathrm{Im}(s)/V)\left(\frac{z + \mathrm{Im}(s)/V}{z - z_1}\right)^{1/2} F(z, s, k_1)^{1/2} \\ &\quad \cdot \left(\frac{z - z_1}{z + \mathrm{Im}[s]/V}\right)\left(\frac{z - z_3}{z - z_2}\right)\frac{e^{I_{32}(z)}}{T_{32}(z)}. \end{aligned} \tag{2.21}$$

Note that $X^{-}(z_0)$ for z_0 on the branch cut $L_1 \cup L_2 \cup L_3$ can be determined by taking the limit of $X^{-}(z)$ as z approaches z_0 from either side of the branch cut.

Finally, for a specific load $\sigma_{yy}^{-}(x, 0, t) = L_e \Lambda_e(x/a_e, t)$ one can determine $F^{+}(z) = \hat{\bar{\sigma}}_{yy}^{+}(z, 0, s)$, $F^{-}(z) = \hat{\bar{v}}^{-}(z, 0, s)$ from Eqs. (2.15) and (2.21). From $\hat{\bar{v}}^{-} = -\beta_1 A + ipB$ and (2.9), A and B can be determined and thus the Laplace transform of any of the stresses or displacements can be found. In particular, the Laplace transform of the stress intensity factor (SIF) $\overline{K}(s)$ can now be calculated as in [20]. Specifically, one has that

$$\hat{\bar{\sigma}}_{yy}(x, 0, s) \sim \frac{\overline{K}(s)}{\sqrt{\pi}} x^{-1/2} \quad \text{as } x \to 0^{+},$$

$$\text{where } \overline{K}(s) = \frac{e^{-\pi i/4}}{2\pi i}\int_{-\infty}^{\infty} \frac{\hat{\bar{\sigma}}^{-}(\tau, s)}{X^{+}(\tau)} d\tau \quad \text{and} \quad \hat{\bar{\sigma}}^{-}(\tau, s) = L_e a_e \hat{\Lambda}_e(a_e \tau, s). \tag{2.22}$$

3. Calculation of the energy release rate. The energy release rate (ERR) will now be calculated based upon the assumption that a Barenblatt type failure zone exists at the crack tip. Specifically, it is assumed that two loads are acting on the crack

faces: the applied (external) tractions denoted $\sigma_e^-(x, t) = L_e\Lambda_e(x/a_e, t)$ and the cohesive (failure) stresses $\sigma_f^-(x, t) = -L_f\Lambda_f(w(x, t), x/a_f, t)$ acting in a failure zone of length a_f immediately behind the crack tip. The essential features of the Barenblatt model are that $a_f \ll a_e$ and that $K_e + K_f = 0$ where K_e and K_f are the SIF's corresponding to σ_e^- and σ_f^-, respectively. The effect of the failure zone is to cancel the singular stresses ahead of the crack tip and thereby produce a cusp shaped crack profile behind the tip. The resulting mathematical problem is: given $\sigma_e^-(x, t)$ find the "response" stress in the failure zone, σ_f^-, and crack face displacements $u(x, 0, t)$ and $v(x, 0, t)$ for $-\infty < x < 0$ that cancel the stress singularity due to $\sigma_e^-(x, t)$ while maintaining a constant crack speed. The goal is then to compute the time evolution of the energy release rate as described below.

The ERR, $G(t)$ (defined to be the energy flux into the crack tip per unit crack advance), is given by

$$G(t) = \frac{1}{V}\int_{Vt-a_f}^{Vt} \sigma_f^-(x_1 - Vt, t)\dot{u}_2(x_1 - Vt, 0, t)\, dx_1,$$

which in the moving coordinates becomes

$$G(t) = \frac{1}{V}\int_{-a_f}^{0} \sigma_f^-(x, t)\left[\frac{\partial}{\partial t} - V\frac{\partial}{\partial x}\right] v(x, 0, t)\, dx. \tag{3.1}$$

Deriving a closed form expression for (3.1) valid for arbitrary applied tractions $\sigma_e^-(x, t)$ and failure zone constitutive law

$$\sigma_f^-(x, t) = -L_f\Lambda_f\left(v(x, 0, t), \frac{x}{a_f}, t\right) \tag{3.2}$$

requires solving an exceedingly complicated nonlinear boundary value problem. The constitutive law (3.2) models the failure zone response as that of a nonlinear elastic spring, accounting for inhomogeneity and aging. In general the failure zone length, a_f, is dynamically changing and determined by the equation $K_e + K_f = 0$. In the absence of any generally accepted, physically motivated form for $\Lambda_f(\cdot, \cdot, \cdot)$, various ad hoc, artificial models have been introduced and studied in the literature. A discussion of these models is contained in [10].

For the dynamic steady-state problem, it was shown in [27] that a simple closed form expression for G is obtained for the special class of loads

$$\sigma_e^-(x) = L_e \exp(x/a_e) \quad \text{and} \quad \sigma_f^-(x) = -L_f \exp(x/a_f) \quad \text{for } -\infty < x < 0. \tag{3.3}$$

It was argued there that, for $a_f \ll a_e$, the fact that $\sigma_f^-(x, t)$ does not have compact support should have a relatively minor effect on the results provided the essential requirements for the Barenblatt model are still satisfied: $a_f \ll a_e$ and $K_e + K_f = 0$. Furthermore, the two cases (1) L_f constant with $a_f = a_f(V)$ and (2) a_f constant with $L_f = L_f(V)$ were compared quantitatively. It was found that, except for very high crack speeds, the two cases produce nearly identical G vs. V curves. In light of these considerations it is likely that valuable insight into the combined influence that

crack speed, inertia, and viscoelastic properties have upon the rate of convergence to steady-state of the transient $G(t)$ can be obtained from generalizing the analysis of Walton [23] to the transient problem addressed here, the unphysical nature of the failure zone constitutive law (3.3) notwithstanding.

Henceforth, a generalization of the forms (3.3) will be assumed for σ_e^- and σ_f^-. Moreover, time-dependent tractions $\sigma_e^-(x, t)$ will be permitted by taking

$$\sigma_e^-(x, t) = L_e l_e(t) \exp(x/a_e), \qquad -\infty < x < 0, \tag{3.4}$$

where $l_e(t)$ is a dimensionless function of time. As with the steady-state analysis in [23], consideration of the two models, (1) L_f constant with $a_f = a_f(V, t)$ and (2) a_f constant with $L_f = L_f(V, t)$, arises naturally. While case (1) is the more physically compelling, it is mathematically much more complicated owing to the nonlinear manner in which the initially unknown function $a_f(V, t)$ occurs in the problem. In contrast, case (2) is clearly unphysical in a dynamic analysis (e.g., it suggests that information travels with an infinite speed of propagation in the failure zone) but, as shown below, admits an elegant closed form expression for $G(t)$ with the aid of which qualititative and quantitative properties can be easily studied. In light of the steady-state results, it is likely that, except for very high crack speeds, the two cases should exhibit similar long time asymptotic behavior whenever $a_f \ll a_e$. Therefore only the analysis of case (2) is considered here.

Note that (3.4) assumes that the spatial form of the applied stress follows the advancing crack tip. A different loading situation in which the spatial form of the applied stresses remains fixed as the crack tip advances is considered at the end of this section.

With $\sigma_e^-(x, t)$ given by (3.4) and $\sigma_f^-(x, t)$ by

$$\sigma_f^-(x, t) = -L_f l_f(t) \exp(x/a_f), \qquad -\infty < x < 0, \tag{3.5}$$

the appropriate definition for $G(t)$ becomes

$$G(t) = \frac{1}{V} \int_{-\infty}^{0} \sigma_f^-(x, t) \left[\frac{\partial}{\partial t} - V \frac{\partial}{\partial x} \right] v(x, 0, t)\, dx. \tag{3.6}$$

In (3.5) the explicit dependence of $l_f(t)$ upon V has been temporarily suppressed. As shown in [23], it is straightforward to extend the analysis to treat more general loads of the form

$$\sigma^-(x, t) = L(t) \int_0^{\infty} e^{rx/a}\, dh(r)$$

where $h(r)$ is any signed measure for which the integral makes sense. However, for the sake of brevity that development is not included here.

Incorporating (3.5) and (3.6) there results

$$G(t) = I(t) + W(t) \tag{3.7}$$

with

$$I(t) = -L_f l_f(t) \frac{1}{V} \int_{-\infty}^{0} e^{x/a_f} \frac{\partial}{\partial t} v(x, 0, t)\, dx \tag{3.8}$$

and

$$W(t) = L_f l_f(t) \int_{-\infty}^{0} e^{x/a_f} \frac{\partial}{\partial x} v(x, 0, t)\, dx. \tag{3.9}$$

$I(t)$ and $W(t)$ in themselves do not have any direct physical significance but the decomposition (3.7) does provide some insight into the behavior of $G(t)$. In particular, it can be shown that $\lim_{t\to 0} G(t) = \lim_{t\to 0} I(t)$ and $\lim_{t\to\infty} G(t) = \lim_{t\to\infty} W(t)$ whereas $\lim_{t\to 0} W(t) = \lim_{t\to\infty} I(t) = 0$. Thus the short time behavior of $G(t)$ is governed primarily by $I(t)$ and the long time behavior by $W(t)$.

To derive the nondimensional form of the ERR, $G(t)$, first consider the integral

$$g_f(t) = \frac{1}{V} \int_{-\infty}^{0} e^{x/a_f} \left[\frac{\partial}{\partial t} - V\frac{\partial}{\partial x}\right] v(x, 0, t)\, dx. \tag{3.10}$$

If one notes that the inverse Fourier transform of $H(-x)e^{x/a_f}$ is $\frac{i}{2\pi}(p + i/a_f)^{-1}$ and applies Parseval's relation to (3.10) and then applies the Laplace transform to the resulting expression, the Laplace transform $\bar{g}_f(s)$ is found to be

$$\bar{g}_f(s) = \frac{-1}{2\pi i} \int_{-\infty}^{\infty} \left[\frac{s}{V} + ip\right] \hat{\bar{v}}^{-}(p, 0, s) \frac{dp}{p + i/a_f}.$$

In the same manner as in [10] this integral is evaluated by residues where (2.15) and (2.21) determine the form of $\hat{\bar{v}}^{-}$. A key step in this derivation is the determination of $\bar{l}_f(s)$ from the Barenblatt hypothesis, which results in the identity

$$\frac{L_e \bar{l}_e(s)}{X^{+}(i/a_e)} = \frac{L_f \bar{l}_f(s)}{X^{+}(i/a_f)}. \tag{3.11}$$

It is then found that

$$\bar{g}_f(s) = \frac{L_e \bar{l}_e(s)}{2} \left[\frac{s}{V} + \frac{1}{a_f}\right] \frac{a_f(a_e - a_f)}{(a_e + a_f)} \frac{X^{-}(-i/a_f)}{X^{+}(i/a_e)}. \tag{3.12}$$

In order to present the results in a nondimensional form, it is necessary to introduce certain parameters. First, a nondimensional shear modulus is defined by $\mu(t) = \mu_\infty m(t/\tau)$ where $\mu_\infty = \lim_{t\to\infty} \mu(t)$ and thus $\lim_{t\to\infty} m(t) = 1$. The parameter τ represents a characteristic relaxation time of the material. The glassy shear wave speed, the glassy longitudinal wave speed, the equilibrium shear wave speed, and the equilibrium longitudinal wave speed are defined by $c_T^2 = \mu(0)/\rho$, $c_L^2 = [\lambda(0) + 2\mu(0)]/\rho$, $c_T^{*2} = \mu_\infty/\rho$, and $c_L^{*2} = [\lambda_\infty + 2\mu_\infty]/\rho$ respectively. Recall that the only nonzero solution of $R(x) = 0$ where $R(x)$ is defined by (2.19) is $x = r_0$ where $0 < r_0 < 1$. If $x = (V/c_T)^2$ then $R((V/c_T)^2) = 0$ is recognized to be the elastic Rayleigh equation and its nonzero solution $V = c_R = \sqrt{r_0}(c_T)$ is called the glassy Rayleigh wave speed; that is, it corresponds to the Rayleigh wave speed for an elastic body with Lamé constants equal to the initial viscoelastic values. Similarly, the equilibrium Rayleigh wave speed, $c_R^* = \sqrt{r_0}(c_T^*)$, corresponds to the Rayleigh wave speed in an elastic body with Lamé constants $\mu = \mu(\infty)$ and $\lambda = \lambda(\infty)$. Also, the nondimensional parameters γ, ε, α, and ζ_1, ζ_2, ζ_3 are defined by $\gamma = V/c_T^*$, $\varepsilon = a_f/a_e$, $\alpha = c_T^*\tau/a_e$, $\zeta_1 = ia_e z_1$, $\zeta_2 = ia_e z_2$, and $\zeta_3 = ia_e z_3$. Note that $\varepsilon \ll 1$, $\alpha > 0$, and $c_L/c_T = c_L^*/c_T^* = 1/\sqrt{k_1}$.

Substituting these nondimensional parameters into (3.12) and (2.21), it is found that $\bar{g}_f(s)$ can be rewritten in nondimensional form as

$$\bar{g}_f(s) = \frac{-L_e a_e \bar{l}_e(s)}{8\mu_\infty} \frac{(1-\varepsilon)}{(1+\varepsilon)} \frac{\gamma^2\sqrt{\varepsilon}}{[\tilde{m}(\tau s + \alpha\gamma/\varepsilon)]^2} \frac{(1-\varepsilon\zeta_1)^{1/2}}{(1+\zeta_1)^{1/2}} \frac{(1+\zeta_2)}{(1-\varepsilon\zeta_2)} \frac{(1-\varepsilon\zeta_3)}{(1+\zeta_3)} \frac{F}{T} e^{I_1 - I_2} \tag{3.13}$$

where

$$F = \left[\left(\frac{\alpha\gamma/\varepsilon}{\tau s + \alpha\gamma/\varepsilon} \right)^2 - \frac{\gamma^2 k_1}{\tilde{m}(\tau s + \alpha\gamma/\varepsilon)} \right]^{1/2},$$

$$T = \left(\frac{\frac{\alpha\gamma}{\varepsilon}}{\tau s + \frac{\alpha\gamma}{\varepsilon}} \right)^2 F \left[\left(\frac{\frac{\alpha\gamma}{\varepsilon}}{\tau s + \frac{\zeta\gamma}{\varepsilon}} \right)^2 - \frac{\gamma^2}{\tilde{m}(\tau s + \frac{\alpha\gamma}{\varepsilon})} \right]^{1/2} - \left[\left(\frac{\frac{\alpha\gamma}{\varepsilon}}{\tau s + \frac{\alpha\gamma}{\varepsilon}} \right)^2 - \frac{(1/2)\gamma^2}{\tilde{m}(\tau s + \frac{\alpha\gamma}{\varepsilon})} \right]^2,$$

$$I_1 = I_n(-1/\varepsilon), \quad I_2 = I_n(1), \quad \text{where } I_n(x) = \frac{\zeta_2 - \zeta_1}{2\pi i} \int_0^1 \frac{\log(T_p(t)) - \log(T_n(t))}{\zeta_1 + t(\zeta_2 - \zeta_1) + x}\, dt,$$

$$F_n(t, k) = \left(\frac{\alpha\gamma[\zeta_1 + t(\zeta_2 - \zeta_1)]}{\tau s + \alpha\gamma[\zeta_1 + t(\zeta_2 - \zeta_1)]} \right)^2 - \frac{\gamma^2 k}{\tilde{m}(\tau s + \alpha\gamma[\zeta_1 + t(\zeta_2 - \zeta_1)])},$$

$$T_p(t) = \left(\frac{\alpha\gamma[\zeta_1 + t(\zeta_2 - \zeta_1)]}{\tau s + \alpha\gamma[\zeta_1 + t[\zeta_2 - \zeta_1)]} \right)^2 |F_n(t, k_1)|^{1/2} e^{(1/2)i \arg(F_n(t, k_1))} |F_n(t, 1)|^{1/2}$$
$$\times e^{(1/2)i \arg^+(F_n(t,1))} - [F_n(t, 1/2)]^2,$$

$$T_n(t) = \left(\frac{\alpha\gamma[\zeta_1 + t(\zeta_2 - \zeta_1)]}{\tau s + \alpha\gamma[\zeta_1 + t[\zeta_2 - \zeta_1)]} \right)^2 |F_n(t, k_1)|^{1/2} e^{(1/2)i \arg(F_n(t, k_1))} |F_n(t, 1)|^{1/2}$$
$$\times e^{-\pi i} e^{(1/2)i \arg^+(F_n(t,1))} - [F_n(t, 1/2)]^2,$$

where $-\pi < \arg(F_n(t, k_1)) \le \pi$, and $0 \le \arg^+(F_n(t, 1)) < 2\pi$.

Attention will now be turned to $l_f(t)$. It follows from (2.21) and (3.11) that

$$\bar{l}_f(s) = \bar{l}_e(s) \frac{L_e}{L_f\sqrt{\varepsilon}} \frac{(1+\varepsilon\zeta_1)^{1/2}}{(1+\zeta_1)^{1/2}} \frac{(1+\zeta_2)}{(1+\varepsilon\zeta_2)} \frac{(1+\varepsilon\zeta_3)}{(1+\zeta_3)} e^{I_3 - I_2}, \tag{3.14}$$

where $I_3 = I_n(1/\varepsilon)$. Finally, utilizing (3.4)–(3.6), (3.13), and (3.14) one may write the ERR as

$$G(t) = -L_f l_f(t) g_f(t) = \frac{L_e^2 a_e}{8\mu_\infty} l(t) g(t), \tag{3.15}$$

where the Laplace transforms of $l(t)$ and $g(t)$ are given by

$$\bar{l}(s) = \bar{l}_e(s) \frac{(1+\varepsilon\zeta_1)^{1/2}}{(1+\zeta_1)^{1/2}} \frac{(1+\zeta_2)}{(1+\varepsilon\zeta_2)} \frac{(1+\varepsilon\zeta_3)}{(1+\zeta_3)} e^{I_3 - I_2}, \tag{3.16}$$

$$\bar{g}(s) = \bar{l}_e(s) \frac{(1-\varepsilon)}{(1+\varepsilon)} \frac{\gamma^2}{[\tilde{m}(\tau s + \alpha\gamma/\varepsilon)]^2} \frac{(l-\varepsilon\zeta_1)^{1/2}}{(1+\zeta_1)^{1/2}} \frac{(1+\zeta_2)}{(1-\varepsilon\zeta_2)} \frac{(1-\varepsilon\zeta_3)}{(1+\zeta_3)} \frac{F}{T} e^{I_1 - I_2}. \tag{3.17}$$

Note that (3.14) and (3.17) have implicitly assumed that $-i/a_f$ does not lie on the branch cut $L_1 \cup L_2 \cup L_3$. This certainly is the case if $\varepsilon < 1/|\zeta_3|$. The only case of

interest where $-i/a_f$ may lie on this branch cut is when s is real and $\varepsilon > 1/\zeta_3$. In this case slight modifications of (3.17) must be made. If $\varepsilon > 1/\zeta_3$ and $\varepsilon \neq 1/\zeta_1, 1/\zeta_2$ then the terms

$$(1-\varepsilon\zeta_1)^{1/2}\frac{(1-\varepsilon\zeta_3)}{(1-\varepsilon\zeta_2)}\frac{F}{T}$$

in (3.17) are replaced by

$$|1-\varepsilon\zeta_1|^{1/2}\frac{|1-\varepsilon\zeta_3|}{|1-\varepsilon\zeta_2|}\frac{|F|}{|T|}.$$

Furthermore, if $1/\zeta_2 < \varepsilon < 1/\zeta_1$ then I_1 in (3.17) should be interpreted as the Cauchy principal value of the integral.

Unfortunately, it is not possible in general to invert (3.16) and (3.17) analytically. Therefore to obtain a better understanding of $G(t)$ both an asymptotic analysis based on (3.15)–(3.17) that is valid for any shear modulus $\mu(t)$ and numerical inversion of the Laplace transforms (3.16) and (3.17) for specific $\mu(t)$ are presented. The asymptotic analysis and the consideration of special cases are addressed in the next section. Numerical inversion of (3.16) and (3.17) for the standard linear solid model of $\mu(t)$ is discussed in the section following the asymptotic analysis.

Most experimental work on dynamic fracture has considered either brittle elastic or ductile materials. Comparatively little data is available for viscoelastic materials. One notable exception is the very careful and extensive investigations found in [13–16]. With minor modifications, our model may shed light on their observations. Their experimental studies of dynamic crack propagation considered an edge crack in a large panel which at $t = 0$ had a constant load applied to a fixed part of the crack faces. The initial acceleration phase of the crack was too short to measure and the crack was observed to rapidly propagate away from the external tractions. Thus the applied tractions did not travel with the advancing crack tip. The preceding model assumed a spatial form for the external tractions that followed the advancing crack tip. Thus, in an effort to model, in a qualitative and idealized manner, the experiments of Ravi-Chandar and Knauss, the spatial form of the external tractions will now be assumed to remain fixed in the fixed coordinate system, i.e.,

$$\sigma_e(x_1, t) = L_e l_e(t)\exp(x_1/a_e), \qquad -\infty < x_1 < 0, \tag{3.18}$$

while the response tractions of the failure zone are still given by (3.5) and hence travel along with the advancing crack tip. While the definition of $G(t)$, (3.6), remains unchanged, the new form of σ_e results in a different Laplace transform of the SIF. This causes the following change to (3.11) (assuming $l_e(t)$ to be constant)

$$\frac{L_e}{s - V/a_e}\left[\frac{1}{X^+(i/a_e)} - \frac{1}{X^+(is/V)}\right] = \frac{L_f \bar{l}_f(s)}{X^+(i/a_f)}. \tag{3.19}$$

The ERR can then be written as

$$G_K(t) = \frac{-L_f l_f(t)}{V} g_f(t),$$

where $\bar{l}_f(s)$ is determined from (3.19) and

$$\bar{g}_f(s) = \frac{L_e}{2}\frac{(s+V/a_f)}{(s-V/a_e)}X^-(-i/a_f)\left[\frac{a_f(a_e-a_f)}{(a_e+a_f)X^+(i/a_e)} + \frac{a_f(s-V/a_f)}{(s+V/a_f)X^+(is/V)}\right]. \tag{3.20}$$

In nondimensional form this becomes

$$G_K(t) = \frac{L_e^2 a_e}{8\mu_\infty} l_K(t) g_K(t),$$

where the Laplace transforms of $l_K(t)$ and $g_K(t)$ are given by

$$\bar{l}_K(s) = \frac{\tau(1+\varepsilon\zeta_1)^{1/2}}{(\tau s-\alpha\gamma)}\frac{(1+\varepsilon\zeta_3)}{(1+\varepsilon\zeta_2)}e^{I_3}\left[\frac{1}{(1+\zeta_1)^{1/2}}\frac{(1+\zeta_2)}{(1+\zeta_3)}e^{-I_2} - \frac{1}{(\frac{\tau s}{\alpha\gamma}+\zeta_1)^{1/2}}\frac{(\frac{\tau s}{\alpha\gamma}+\zeta_2)}{(\frac{\tau s}{\alpha\gamma}+\zeta_3)}e^{-I_4}\right] \tag{3.21}$$

$$\bar{g}_K(s) = \frac{\tau\gamma^2}{[\tilde{m}(\tau s+\alpha\gamma/\varepsilon)]^2}\frac{(1-\varepsilon\zeta_1)^{1/2}}{(\tau s-\alpha\gamma)}\frac{(1-\varepsilon\zeta_3)}{(1-\varepsilon\zeta_2)}\frac{F}{T}e^{I_1} \cdot\left[\frac{(1-\varepsilon)}{(1+\varepsilon)}\frac{1}{(1+\zeta_1)^{1/2}}\frac{(1+\zeta_2)}{(1+\zeta_3)}e^{-I_2} + \frac{(\tau s-\alpha\gamma/\varepsilon)}{(\tau s+\alpha\gamma/\varepsilon)}\frac{1}{(\frac{\tau s}{\alpha\gamma}+\zeta_1)^{1/2}}\frac{(\frac{\tau s}{\alpha\gamma}+\zeta_2)}{(\frac{\tau s}{\alpha\gamma}+\zeta_3)}e^{-I_4}\right], \tag{3.22}$$

where $I_4 = I_n(\frac{\tau s}{\alpha\gamma})$.

The results of asymptotic and sample numerical investigations of this ERR, $G_K(t)$, also appear in the next section.

4. Special cases and asymptotic solutions. Asymptotic expansions for the ERR, $G(t)$, as $t \to 0$ and as $t \to \infty$ can now be constructed from (3.15)–(3.17). Specifically, asymptotic expansions for $l(t)$ and $g(t)$ are constructed separately and multiplied together. Henceforth, unless indicated to the contrary, attention will be limited to the special case $l_e(t) = 1$, i.e., the external tractions driving the crack will be assumed to be time independent. In that case $\bar{l}_e(s) = 1/s$. More general time dependence for $l_e(t)$ is easily incorporated into $l(t)$ and $g(t)$ as a simple convolution.

Asymptotic behavior as $t \to 0$. Though a short time approximation of $G(t)$ may be of dubious physical significance, it does provide a valuable check on the numerical Laplace inversion performed in the next section. In a manner analogous to that in [10], it can be shown that

$$\zeta_n(s) = h_n s + o(s) \quad \text{as } s \to \infty, \tag{4.1}$$

where

$$h_1 = \frac{\tau}{\alpha[(c_L/c_L^*)-\lambda]}, \quad h_2 = \frac{\tau}{\alpha[(c_T/c_T^*)-\gamma]}, \quad h_3 = \frac{\tau}{\alpha[(c_R/c_T^*)-\gamma]}.$$

Asymptotic expansion of $\bar{l}(s)$ and $\bar{g}(s)$ in powers of $\frac{1}{s}$ as $s \to \infty$ are given by

$$\bar{l}(s) = \frac{1}{s}\sqrt{\varepsilon}\left[1 + \frac{(1-\varepsilon)}{\varepsilon}\frac{1}{s}\left(\frac{1}{2h_1}+\frac{1}{h_3}-\frac{1}{h_2}+A_0\right)+o(s^{-1})\right], \tag{4.2}$$

$$\bar{g}(s) = \frac{(1-\varepsilon)}{(1+\varepsilon)}\left(\frac{\varepsilon k_1}{m(0)}\right)^{1/2}\frac{4}{\gamma s}\left\{1 - \frac{1}{s}\left[\frac{(1+\varepsilon)}{\varepsilon}\left(\frac{1}{2h_1}+\frac{1}{h_3}-\frac{1}{h_2}+A_0\right)+\frac{m'(0)}{2\tau m(0)}\right] + o(s^{-1})\right\} \tag{4.3}$$

where

$$A_0 = \frac{h_2-h_1}{\pi}\int_0^1 \frac{\tan^{-1}(A(t))}{[h_1+t(h_2-h_1)]^2}\,dt,$$

$$A(t) = \frac{f(t)[f(t)-\gamma^2 k_1/m(0)]^{1/2}|f(t)-\gamma^2/m(0)|^{1/2}}{[f(t)-(1/2)\gamma^2/m(0)]^2},$$

$$f(t) = \frac{\{\alpha\gamma[h_1+t(h_2-h_1)]\}^2}{\{\tau+\alpha\gamma[h_1+t(h_2-h_1)]\}^2}.$$

If one assumes that $l(t)$ and $g(t)$ have Maclaurin expansions in a neighborhood of $t=0$, then from (4.2), (4.3), (3.15), and standard asymptotic results for the Laplace transform,

$$G(t) = \frac{L_e^2 a_e}{2\gamma\mu_\infty}\frac{(1-\varepsilon)}{(1+\varepsilon)}\varepsilon\left(\frac{k_1}{m(0)}\right)^{1/2}[1-at+o(t)] \quad \text{as } t\to 0, \tag{4.4}$$

where

$$a = 2\left(\frac{1}{2h_1}+\frac{1}{h_3}-\frac{1}{h_2}+A_0\right)+\frac{m'(0)}{2\tau m(0)}.$$

In agreement with the mode III crack in [10], $G(t)$, for t near zero, is governed by the glassy properties except for the inclusion of the term $m'(0)$ which incorporates the effect of the initial rate of stress relaxation.

In contrast, the asymptotic expansions of $l_K(s)$ and $g_K(s)$ as $s\to\infty$ are

$$\bar{l}_K(s) = \frac{1}{s}\sqrt{\varepsilon}\left[1-\frac{\sqrt{h_1}}{\sqrt{\frac{\tau}{\alpha\gamma}+h_1}}\frac{h_3}{h_2}\frac{(\frac{\tau}{\alpha\gamma}+h_2)}{(\frac{\tau}{\alpha\gamma}+h_3)}e^{-A_1}\right]+o(s^{-1}), \tag{4.5}$$

$$\bar{g}_K(s) = \left(\frac{\varepsilon k_1}{m(0)}\right)^{1/2}\frac{4}{\gamma s}\left[\frac{(1-\varepsilon)}{(1+\varepsilon)}-\frac{\sqrt{h_1}}{\sqrt{\frac{\tau}{\alpha\gamma}+h_1}}\frac{h_3}{h_2}\frac{(\frac{\tau}{\alpha\gamma}+h_2)}{(\frac{\tau}{\alpha\gamma}+h_3)}e^{-A_1}\right]+o(s^{-1}), \tag{4.6}$$

where

$$A_1 = \frac{h_2-h_1}{\pi}\int_0^1 \frac{\tan^{-1}(A(t))}{[h_1+t(h_2-h_1)][h_1+t(h_2-h_1)+\frac{\tau}{\alpha\gamma}]}\,dt.$$

Thus

$$G_K(t) = \frac{L_e^2 a_e \varepsilon}{2\gamma\mu_\infty}\left(\frac{k_1}{m(0)}\right)^{1/2}\left[1-\frac{\sqrt{h_1}}{\sqrt{\frac{\tau}{\alpha\gamma}+h_1}}\frac{h_3}{h_2}\frac{(\frac{\tau}{\alpha\gamma}+h_2)}{(\frac{\tau}{\alpha\gamma}+h_3)}e^{-A_1}\right] \cdot\left[\frac{(1-\varepsilon)}{(1+\varepsilon)}-\frac{\sqrt{h_1}}{\sqrt{\frac{\tau}{\alpha\gamma}+h_1}}\frac{h_3}{h_2}\frac{(\frac{\tau}{\alpha\gamma}+h_2)}{(\frac{\tau}{\alpha\gamma}+h_3)}e^{-A_1}\right]+o(1) \quad \text{as } t\to 0. \tag{4.7}$$

Asymptotic behavior as $t \to \infty$. To determine the long-time asymptotic behavior of $G(t)$, i.e., $\lim_{t\to\infty} G(t)$, it is necessary to calculate $\lim_{s\to 0} s\bar{l}(s)$ and $\lim_{s\to 0} s\bar{g}(s)$. Again in a manner analogous to [10] it can be shown that as $s \to 0$

$$\begin{aligned} \zeta_n &= a_n s + o(s) \quad \text{for } \gamma < \lambda_n, \\ \zeta_n &= b_n s^{1/2} + o(s^{1/2}) \quad \text{for } \gamma = \lambda_n, \\ \zeta_n &= c_n + o(1) \quad \text{for } \gamma > \lambda_n \end{aligned} \tag{4.8}$$

where

$$a_n = \frac{\tau}{\alpha[\lambda_n - \gamma]}, \qquad b_n = \frac{\sqrt{2\tau}}{\alpha\gamma}\left[-\int_0^\infty r m'(r)\, dr\right]^{-1/2},$$

$$c_n \text{ is defined implicitly by } \frac{\gamma^2}{\lambda_n^2} - m(0) = \int_0^\infty e^{-\alpha\gamma c_n r} m'(r)\, dr$$

for $n = 1, 2, 3$ and $\lambda_1 = 1/\sqrt{k_1}$, $\lambda_2 = 1$, and $\lambda_3 = \sqrt{r_0}$. Then

$$\lim_{t\to\infty} G(t) = \frac{L_e^2 a_e}{8\mu_\infty}\frac{(1-\varepsilon)}{(1+\varepsilon)}\frac{\gamma^2}{[\tilde{m}(\alpha\gamma/\varepsilon)]^2}\frac{|F_\infty(\alpha\gamma/\varepsilon, k_1)|^{1/2}}{T_\infty} g_c, \tag{4.9}$$

where

$$F_\infty(x, k) = 1 - \frac{k\gamma^2}{\tilde{m}(x)},$$

$$T_\infty = |F_\infty(\alpha\gamma/\varepsilon, k_1)^{1/2} F_\infty(\alpha\gamma/\varepsilon, 1)^{1/2} - F_\infty(\alpha\gamma/\varepsilon, 1/2)^2|,$$

and

$$g_c = \begin{cases} 1, & \text{if } \gamma \le \sqrt{r_0}\ (V \le c_R^*); \\ \frac{|1-(\varepsilon c_3)^2|}{(1+c_3)^2}, & \text{if } \sqrt{r_0} < \gamma \le 1\ (c_R^* < V \le c_T^*); \\ \frac{|1-(\varepsilon c_3)^2|}{(1+c_3)^2}\frac{(1+c_2)^2}{|1-(\varepsilon c_2)^2|} e^{J_1+J_3-2J_2}, & \text{if } 1 < \gamma \le 1/\sqrt{k_1}\ (c_T^* < V \le c_L^*); \\ \frac{(1+c_2)^2}{|1-(\varepsilon c_2)^2|}\frac{|1-(\varepsilon c_1)^2|^{1/2}}{1+c_1} e^{K_1+K_3-2K_2}, & \text{if } 1/\sqrt{k_1} < \gamma \le c_R/c_T^*\ (c_L^* < V \le c_R), \end{cases}$$

where $J_1 = J(-1/\varepsilon)$, $J_2 = J(1)$, $J_2 = J(1/\varepsilon)$,

$$J(x) = \frac{c_2}{\pi}\int_0^1 \frac{\tan^{-1} B(t)}{tc_2 + x}\, dt, \qquad B(t) = \frac{F_\infty(t\alpha\gamma c_2, k_1)^{1/2}|F_\infty(t\alpha\gamma c_2, 1)|^{1/2}}{-F_\infty(t\alpha\gamma c_2, 1/2)^2},$$

$$K_1 = K(-1/\varepsilon), \qquad K_2 = K(1), \qquad K_3 = K(1/\varepsilon),$$

$$K(x) = \frac{c_2 - c_1}{\pi}\int_0^1 \frac{\tan^{-1} C(t)}{c_1 + t(c_2 - c_1) + x}\, dt,$$

$$C(t) = \frac{F_\infty(\alpha\gamma[c_1 + t(c_2 - c_1)], k_1)^{1/2}|F_\infty(\alpha\gamma[c_1 + t(c_2 - c_1)], 1)|^{1/2}}{-F_\infty(\alpha\gamma[c_1 + t(c_2 - c_1)], 1/2)^2}.$$

Note that if $\varepsilon > 1/c_2$ when $1 < \gamma \le 1/\sqrt{k_1}$ then J_1 is to be interpreted as a Cauchy principal value and that if $1/c_2 < \varepsilon < 1/c_3$ when $1/\sqrt{k_1} < \gamma \le c_R/c_T^*$ then K_1 is

to be interpreted as a Cauchy principal value. These limits as $t \to \infty$ can be seen to agree with the steady-state results found in [24].

For the loading given by (3.18) with $l_e(t) = 1$, it is found that for $\gamma < \sqrt{r_0}$ as $s \to 0$,

$$g_K(s) = \frac{\tau\gamma}{\alpha} s^{-1/2} \frac{1}{[\tilde{m}(\alpha\gamma/\varepsilon)]^2} \frac{|F_\infty(\alpha\gamma/\varepsilon, k_1)|^{1/2}}{T_\infty(\frac{\tau}{\alpha\gamma} + a_1)^{1/2}} \frac{(\frac{\tau}{\alpha\gamma} + a_2)}{(\frac{\tau}{\alpha\gamma} + a_3)} e^{I_\infty} + o(s^{-1/2}),$$
$$l_K(s) = \frac{\tau}{\alpha\gamma} s^{-1/2} \frac{1}{(\frac{\tau}{\alpha\gamma} + a_1)^{1/2}} \frac{(\frac{\tau}{\alpha\gamma} + a_2)}{(\frac{\tau}{\alpha\gamma} + a_3)} e^{I_\infty} + o(s^{-1/2}) \tag{4.10}$$

where

$$I_\infty = \frac{a_2 - a_1}{\pi} \int_0^1 \frac{\tan^{-1} D(t)}{a_1 + t(a_2 - a_1) + \frac{\tau}{\alpha\gamma}} dt,$$
$$D(t) = \frac{d(t)^2 \left[d(t)^2 - \frac{k_1\gamma^2}{\tilde{m}(x)}\right]^{1/2} \left[d(t)^2 - \frac{\gamma^2}{\tilde{m}(x)}\right]^{1/2}}{\left[d(t)^2 - \frac{\frac{1}{2}\gamma^2}{\tilde{m}(x)}\right]^2},$$
$$d(t) = \frac{\alpha\gamma[a_1 + t(a_2 - a_1)]}{\tau + \alpha\gamma[a_1 + t(a_2 - a_1)]}.$$

Thus it can be seen that $\lim_{s\to 0} s l_K(s) = 0$ and $\lim_{s\to 0} s g_K(s) = 0$ and therefore $\lim_{t\to\infty} G_K(t) = 0$. Furthermore, from the fact that $l_K(s)$ and $g_K(s)$ are $O(s^{-1/2})$ as $s \to 0$ it can be shown that $l_K(t)$ and $g_K(t)$ are $O(t^{-1/2})$ as $t \to \infty$. Thus $G_K(t) = O(t^{-1})$ as $t \to \infty$ for $\gamma < \sqrt{r_0}$. If $\sqrt{r_0} \le \gamma \le c_R/c_T^*$ then $l_K(t)$ and $g_K(t)$ each decay to zero even faster than $O(t^{-1/2})$ with the decay becoming exponential for $1/\sqrt{k_1} < \gamma \le c_R/c_T^*$.

It should be noted that while the above asymptotic analysis for $G_K(t)$ showed that $\lim_{t\to\infty} G_K(t) = 0$ for a load which remained constant in time, i.e., $l_e(t) = 1$, that loads which increase fast enough as time passes, e.g., $l_e(t) = t$, have $\lim_{t\to\infty} G_K(t) = \infty$.

Elastic material model. If the shear modulus is set to be constant, i.e. $\mu(t) = \mu_0$, then the material is modeled as an elastic solid with Lamé moduli equal to the initial glassy values. In this case only three wave speeds are possible, c_R, c_T, and c_L. Furthermore, ζ_1, ζ_2, and ζ_3 can be determined explicitly to be

$$\zeta_1 = \frac{a_e s}{c_L - V}, \quad \zeta_2 = \frac{a_e s}{c_T - V}, \quad \zeta_3 = \frac{a_e s}{c_R - V}. \tag{4.11}$$

Moreover, in the definitions of F, T, and F_n for (3.16), $\gamma^2/\tilde{m}(\cdot)$ should be replaced by $(V/c_T)^2$. Then the ERR for an elastic material is given by

$$G_{\text{el}}(t) = \frac{L_e^2 a_e}{8\mu_0} l(t) g_{\text{el}}(t), \tag{4.12}$$

where

$$\bar{g}_{\mathrm{el}}(s) = \bar{l}_e(s)\frac{(1-\varepsilon)}{(1+\varepsilon)}\left[\frac{V}{c_T}\right]^2 \frac{(1-\varepsilon\zeta_1)^{1/2}}{(1+\zeta_1)^{1/2}}\frac{(1+\zeta_2)}{(1-\varepsilon\zeta_2)}\frac{(1-\varepsilon\zeta_3)}{(1+\zeta_3)}\frac{F}{T}e^{I_1-I_2} \tag{4.13}$$

and $\bar{l}(s)$ is given by (3.16) with ζ_1, ζ_2, and ζ_3 in these formulas given by (4.11). Again it is assumed in (4.9) that $-i/a_f$ does not lie on the branch cut $L_1 \cup L_2 \cup L_3$ or modifications similar to those for (3.17) are necessary.

Similarly, for the loading (3.18) which models the Ravi-Chandar and Knauss experiments,

$$G_{K\,\mathrm{el}}(t) = \frac{L_e^2 a_e}{8\mu_0} l_K(t) g_{K\,\mathrm{el}}(t), \tag{4.14}$$

where

$$\bar{g}_{K\,\mathrm{el}}(s) = \tau\left[\frac{V}{c_T}\right]^2 \frac{(1-\varepsilon\zeta_1)^{1/2}}{(\tau s-\alpha\gamma)}\frac{(1-\varepsilon\zeta_3)}{(1-\varepsilon\zeta_2)}\frac{F}{T}e^{I_1} \cdot\left[\frac{(1-\varepsilon)}{(1+\varepsilon)}\frac{1}{(1+\zeta_1)^{1/2}}\frac{(1+\zeta_2)}{(1+\zeta_3)}e^{-I_2}+\frac{(\tau s-\alpha\gamma/\varepsilon)}{(\tau s+\alpha\gamma/\varepsilon)}\frac{1}{(\frac{\tau s}{\alpha\gamma}+\zeta_1)^{1/2}}\frac{(\frac{\tau s}{\alpha\gamma}+\zeta_2)}{(\frac{\tau s}{\alpha\gamma}+\zeta_3)}e^{-I_4}\right] \tag{4.15}$$

and $\bar{l}_K(s)$ is given by (3.21) with ζ_1, ζ_2, and ζ_3 in these formulas given by (4.11) and $\gamma^2/\tilde{m}(\cdot)$ in the definitions of F, T, and F_n replaced by $(V/c_T)^2$.

Quasi-static viscoelastic crack propagation. If the limit of (3.16) and (3.17) is taken as $\rho \to 0$, then the ERR for a quasi-statically propagating crack in a viscoelastic material may be determined. It can be shown that $\zeta_1 = \zeta_2 = \zeta_3 = 0$ and hence that

$$G_q(t) = \frac{L_e^2 a_e}{8\mu_\infty} l_e(t) g_q(t), \tag{4.16}$$

where

$$\bar{g}_q(s) = 2\bar{l}_e(s)\frac{(1-\varepsilon)}{(1+\varepsilon)}\frac{1}{(1-k_1)}\frac{1}{\tilde{m}(\tau s+V\tau/a_f)}(1+sa_f/V). \tag{4.17}$$

It is easily seen that if k_1 were set to $1/2$, then (4.16)–(4.17) are identical to the mode III quasi-static ERR found in [10]. Also, it can be seen in (4.17) that for $l_e(t) = 1$, $g_q(t)$ exhibits a Dirac delta singularity at $t = 0$.

Similarly, the quasi-static limit of (3.21)–(3.22) is found to be

$$G_{Kq}(t) = \frac{L_e^2 a_e}{8\mu_\infty} l_{Kq}(t) g_{Kq}(t), \tag{4.18}$$

where

$$\bar{g}_{Kq}(s) = \frac{2}{\tilde{m}(\tau s+V\tau/a_f)}\frac{(1+sa_f/V)}{(s-V/a_e)}\frac{1}{(1-k_1)}\left[\frac{(1-\varepsilon)}{(1+\varepsilon)}+\frac{(s-V/a_f)}{(s+V/a_f)}\frac{1}{(sa_e/V)^{1/2}}\right],$$

$$\bar{l}_{Kq}(s) = \frac{1}{(s-V/a_e)}\left[1-\frac{1}{(sa_e/V)^{1/2}}\right]. \tag{4.19}$$

No failure zone. If the limit of (3.16)–(3.17) is taken as $\varepsilon \to 0$, then the ERR for the case of no failure zone can be determined. It is found that $G(t)$ becomes

$$G_{\mathrm{nf}}(t) = \frac{L_e^2 a_e}{8\mu_0} l_{\mathrm{nf}}(t) g_{\mathrm{nf}}(t), \tag{4.20}$$

where

$$\begin{aligned} \bar{g}_{\mathrm{nf}}(s) &= \bar{l}_e(s) \left[\frac{V}{c_T}\right]^2 (1+\zeta_1)^{-1/2} \frac{(1+\zeta_2)}{(1+\zeta_3)} \frac{F_{\mathrm{nf}}}{T_{\mathrm{nf}}} e^{-I_2}, \\ \bar{l}_{\mathrm{nf}}(s) &= \bar{l}_e(s)(1+\zeta_1)^{-1/2} \frac{(1+\zeta_2)}{(1+\zeta_3)} e^{-I_2}, \end{aligned} \tag{4.21}$$

with $F_{\mathrm{nf}} = [1-(V/c_L)^2]^{1/2}$ and $T_{\mathrm{nf}} = [1-(V/c_L)^2]^{1/2}[1-(V/c_T)^2]^{1/2} - [1-\frac{1}{2}(V/c_T)^2]^2$ and ζ_1, ζ_2, ζ_3, and I_2 are unchanged from their values in (3.16)–(3.17). Thus it can be seen that without a failure zone the viscoelastic effect on the ERR is only through the roots ζ_1, ζ_2, and ζ_3.

Similarly, if the limit of (3.21)–(3.22) is taken as $\varepsilon \to 0$, then the ERR for a constant loading fixed on the crack faces with no failure zone can be determined. It is found that $G_K(t)$ becomes

$$G_{K\,\mathrm{nf}}(t) = \frac{L_e^2 a_e}{8\mu_0} l_{K\,\mathrm{nf}}(t) g_{K\,\mathrm{nf}}(t), \tag{4.22}$$

where

$$\begin{aligned} \bar{g}_{K\,\mathrm{nf}}(s) = \frac{1}{(s - V/a_e)} \left[\frac{V}{c_T}\right]^2 \frac{F_{\mathrm{nf}}}{T_{\mathrm{nf}}} \Bigg[& (1+\zeta_1)^{-1/2} \frac{(1+\zeta_2)}{(1+\zeta_3)} e^{-I_2} \\ & - (a_e s/V + \zeta_1)^{-1/2} \frac{(a_e s/V + \zeta_2)}{(a_e s/V + \zeta_3)} e^{-I_4} \Bigg], \\ \bar{l}_{K\,\mathrm{nf}}(s) = \frac{1}{(s - V/a_e)} \Bigg[& (1-\zeta_1)^{-1/2} \frac{(1+\zeta_2)}{(1+\zeta_3)} e^{-I_2} \\ & - (a_e s/V + \zeta_1)^{-1/2} \frac{(a_e s/V + \zeta_2)}{(a_e s/V + \zeta_3)} e^{-I_4} \Bigg]. \end{aligned} \tag{4.23}$$

5. Numerical examples. While the asymptotic results in the previous section provide clues to the time evolution of the ERR, its complete history can be determined only by inversion of the Laplace transforms $\bar{l}(s)$ and $\bar{g}(s)$ in (3.16) and (3.17) or the Laplace transforms $\bar{l}_K(s)$ and $\bar{g}_K(s)$ in (3.21) and (3.22). The extremely complicated forms of these Laplace transforms make the construction of useful analytical inverses unlikely. Instead, attention will be directed to their numerical inversion. However, numerical Laplace inversion is notoriously unstable and the manner of inversion must be chosen with care. After experimentation with a variety of methods, including a new method based on approximation by sinc functions [2], it was found that a scheme due to Weeks [25] based upon approximating a function by generalized Laguerre functions was by far and away the most stable and accurate. After Laplace inversion, this approximation when restricted to a Bromwich path[1] is seen

[1] A vertical line in the complex plane such that the real part of any point on the line is positive.

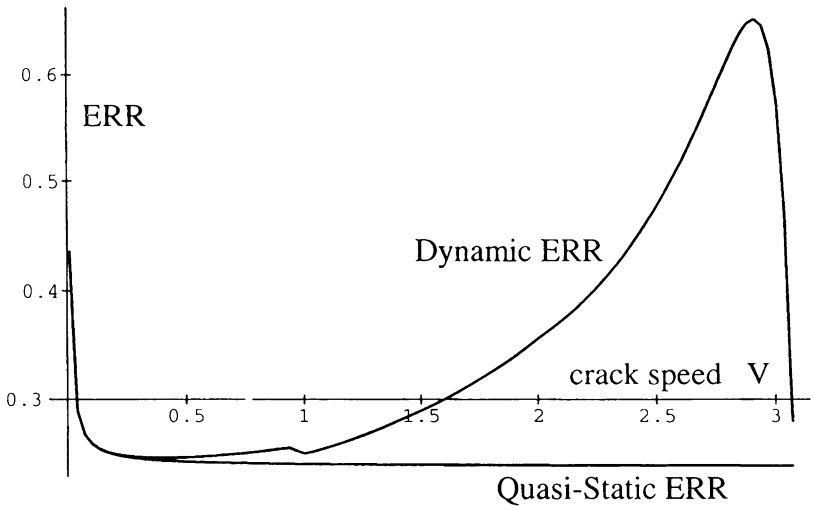

FIG. 1. Comparison of the long time limit of the nondimensionalized dynamic ERR, $G(t)/(L_e^2 a_e/(8\mu_\infty))$, and the nondimensionalized quasi-static ERR, $G_q(t)/(L_e^2 a_e/(8\mu_\infty))$. $\alpha = 1$, $\tau = 1$, $\varepsilon = .01$, $a_e = 1$, $k_1 = .25$ and wave speeds $c_R^* = .93$, $c_T^* = 1.00$, $c_L^* = 2.0$, and $c_R = 3.09$.

to be a Fourier series in the Laplace variable s. By determining the coefficients of a Fourier series of a Laplace transformed function on this Bromwich path, an accurate approximation of the original function by Laguerre functions is obtained. Davies and Martin [7] compared many different numerical Laplace inversion methods and found this method to give "exceptional accuracy on a wide range of functions." This algorithm was employed in the numerical inversion of the examples that follow. However, it was found by numerical experimentation that the optimal parameter value for the algorithm reported in [7] is not correct. Much higher accuracy is obtained by choosing the parameter value so as to get much closer to the singularity of the Laplace transform with greatest real part. In the Laplace transforms considered here the rightmost singularity usually occurs at $s = 0$ and therefore the parameter value was chosen to be .0001.

In the following examples, the viscoelastic material model used is a standard linear solid whose shear modulus is given by $\mu(t) = \mu_\infty(1+\eta e^{-t/\tau})$. Furthermore, only time independent applied tractions are considered, i.e., $l_e(t)$ is assumed to be identically 1.

Figure 1 compares the crack speed dependence of the steady-state values (long time limits) of the nondimensionalized ERRs[2] for a crack propagating dynamically (inertia included) in a viscoelastic material, (4.9), and quasi-statically (ignoring inertia), (4.16)–(4.17). It can be seen for the parameter values selected that the steady-state limits of the ERRs are similar up to about one-half of the equilibrium transverse

[2]In Figs. 1–7, the ERRs have been nondimensionalized by dividing G by $L_e^2 a_e/(8\mu_\infty)$. In Figs. 6 and 7, the viscoelastic ERRs are compared to elastic ERRs where the elastic shear modulus is equal to the viscoelastic glassy shear modulus value.

wave speed. Except for the small local maximum in the steady-state viscoelastic ERR at the equilibrium Rayleigh wave speed, these graphs are qualitatively similar to steady-state mode III results in [11]. Figure 2 shows that even when the steady-state limits of these ERRs are similar, their time histories are quite different. The quasi-static ERR (assuming $l_e(t)$ is constant) has $\lim_{t\to 0} G_q(t) = \infty$ and monotonically decreases to its steady-state value. The dynamic ERR has $G(0)$ finite, although $\lim_{v\to 0} G(0) = \infty$, followed by a quick decrease in the ERR and then a monotonic increase to its steady-state value. This decrease in the dynamic ERR is not visible in Fig. 2 since it happens on an extremely small time scale and is small except for very low crack speeds. It should be noted that these effects near $t = 0$ are due to the assumption that the crack begins to propagate suddenly at $t = 0$ with constant speed and would not be expected to occur if the crack were allowed a reasonable acceleration phase.

Figure 3 compares the time evolution of the transient ERR $G(t)$ for various crack speeds for the case of tractions travelling with the crack tip (formulas (3.15)–(3.17)). It can be seen that the faster the crack speed, the slower the ERR's rate of convergence to its steady state value. Figure 4 (see p. 224) considers the case of tractions that do not move with the crack tip (formulas (3.21) and (3.22)). It can be seen for this case that faster crack speeds lead to lower peak values of the transient ERR $G_K(t)$.

Thus far, the question of selecting a suitable fracture criterion has not been addressed. A commonly adopted fracture criterion is that crack growth be governed by requiring the energy from the applied tractions made available through the continuum to the crack tip process zone be maintained at a critical, constant value, g_{cr}, which is a material parameter independent of crack speed. Figures 1–4 are examples of the time evolution of the available energy assuming that the crack speed is constant.

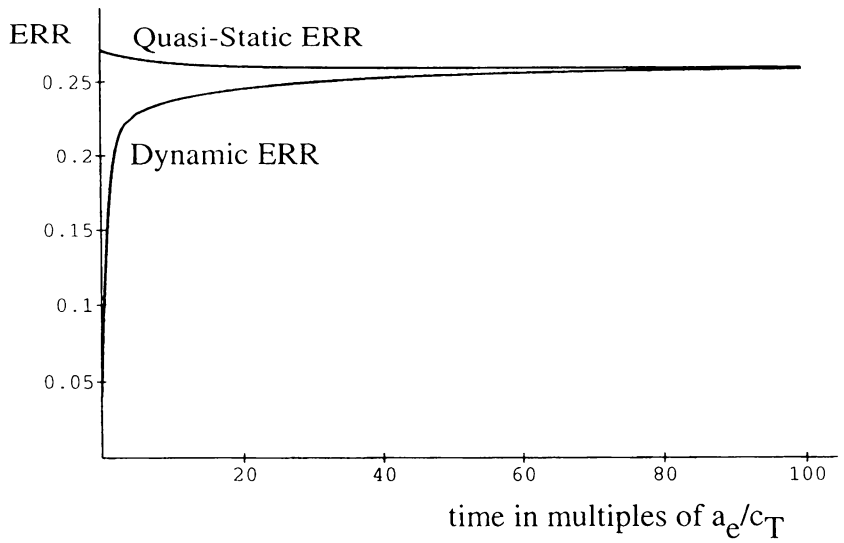

FIG. 2. Comparison of the transient dynamic and quasi-static nondimensionalized ERR, $G(t)/(L_e^2 a_e/(8\mu_\infty))$ and $G_q(t)/(L_e^2 a_e/(8\mu_\infty))$. $\alpha = 1$, $\gamma = 0.1$, $\tau = 1$, $\varepsilon = .01$, $a_e = 1$, $c_T = 3.3166$, and $k_1 = .25$.

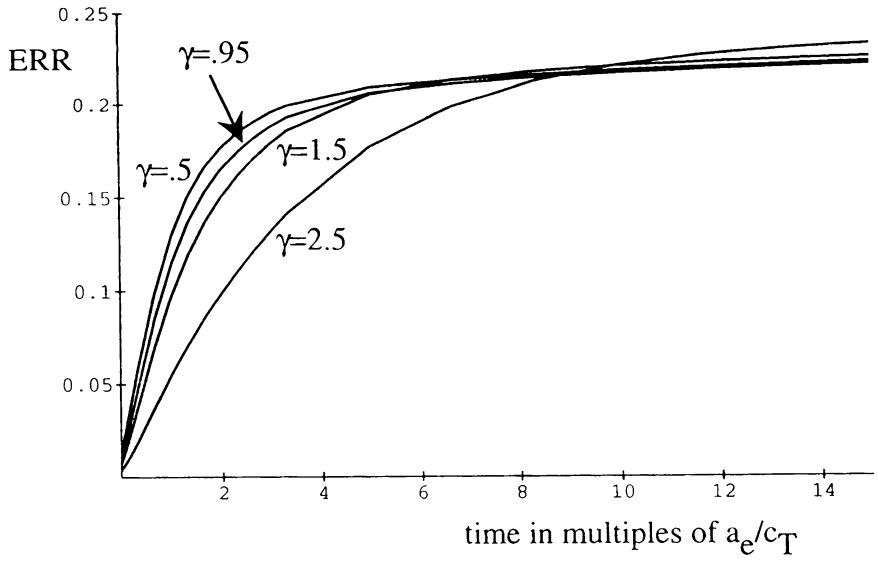

FIG. 3. Comparison of the nondimensionalized dynamic ERR for different crack speeds. $\alpha = 1$, $\tau = 1$, $\varepsilon = .01$, $a_e = 1$, and $k_1 = .25$ with wave speeds $c_R^* = .93$, $c_T^* = 1.00$, $c_L^* = 2.00$, $c_R = 3.09$, and $c_T = 3.32$. The steady state limits are .246 for $\gamma = .5$, .254 for $\gamma = .95$, .289 for $\gamma = 1.5$, and .476 for $\gamma = 2.5$.

Clearly, the available energy is not time constant. One is then led to the conclusion that, for these models, maintaining a constant crack speed and constant energy flow into the crack tip are incompatible. It should be pointed out that changing the crack tip constitutive model to allow the length of the failure zone to change dynamically while the failure zone stress is kept at a constant level (equal to a plastic-type yield stress, for example) does not affect this incompatibility. Indeed, the approximate elastic analyses of Glennie and Willis [8] and Achenbach and Neimitz [1] and some preliminary results of the present authors on accelerating semi-infinite cracks show that the assumption of a constant, critical ERR (required energy) in a Dugdale model with a dynamically changing failure zone length yields a predicted crack tip velocity that is not constant. In particular, if in the Dugdale model the failure zone stress is constant, then the SIF condition determines the time evolution of the failure zone length as a function of the crack tip motion. If a fracture criterion is then specified in the form of matching the rate of work in the Dugdale zone to a required ERR, a nonlinear integral equation emerges governing the crack tip motion. One then finds that the crack tip acceleration is not zero for the case of constant required ERR. Clearly then, one cannot model the experiments of Ravi-Chandar and Knauss, which show constant crack speeds, with a critical (constant) ERR fracture criterion.

It would be interesting to investigate what sort of micromechanical, crack tip model would yield a required ERR equal to the constant crack speed available ERR predicted here. Such an enterprise is beyond the scope of the present paper. However, while a physically realistic fracture criterion appropriate for the Ravi-Chandar and Knauss experiments may be rather complicated, it is reasonable to postulate the exis-

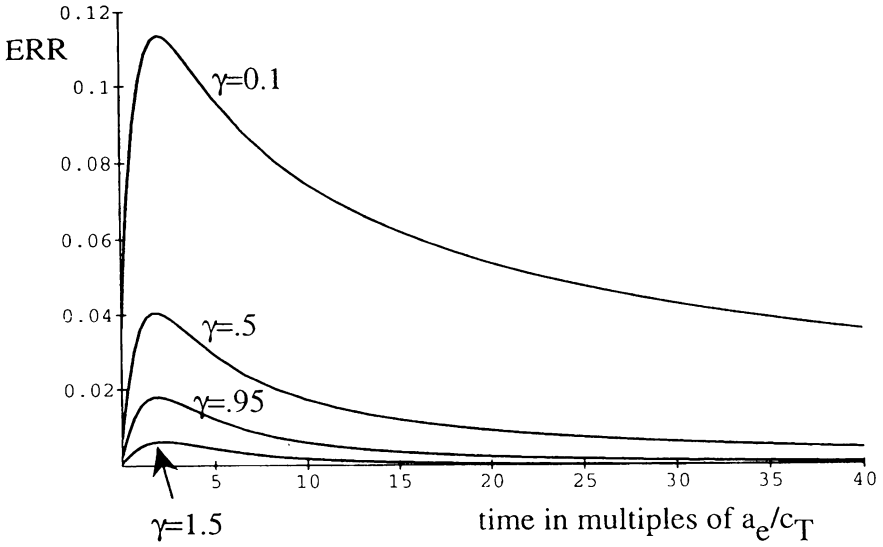

FIG. 4. Comparison of the nondimensionalized dynamic ERR $G_K(t)/(L_e^2 a_e/(8\mu_\infty))$ for different crack speeds. $\alpha = 1$, $\tau = 1$, $\varepsilon = .01$, $a_e = 1$, and $k_1 = .25$ with wave speeds $c_R^* = .93$, $c_T^* = 1.00$, $c_L^* = 2.00$, $c_R = 3.09$, and $c_T = 3.32$.

tence of a minimum required ERR, G_m, for crack growth to occur. Since Fig. 4 plots the available ERR, $G_K(t)$, nondimensionalized by $L_e^2 a_e/\mu_\infty$, one must assume that the applied loading (essentially, L_e) is sufficiently high to ensure that $G_K(0+) \geq G_m$ in order for the crack to begin to propagate at the speed V. (Note that this is similar to the explanation suggested by Ravi-Chandar and Knauss that the initial SIF determines the initial crack speed.) Crack propagation (at the speed V) would cease whenever the available ERR dropped below G_m. There remains the question of what happens to the excess available energy above G_m. A reasonable conjecture has been offered by Ravi-Chandar and Knauss. They observed [15] that the micromechanical structure of the fracture process changed as the stress intensity factor increased even though the crack speed remained the same. In particular, they observed the crack surface changing from a smooth surface to a rougher surface corresponding to more microcracking near the crack tip. Presumably, the excess energy would be consumed by this (time dependent) microcracking process.

Figure 5 shows the result of multiplying the available ERR curve corresponding to $\gamma = 1.5$ in Fig. 4 by a constant in order to produce the same peak value as the curve corresponding to $\gamma = 0.1$. One then sees that the rate of convergence of the $\gamma = 1.5$ curve to zero is much faster than the $\gamma = 0.1$ curve. This suggests that a fast moving crack would be expected to stop (or at least begin to slow down) sooner than a slower moving crack. However, while the faster moving crack may stop sooner, the extent of crack growth for the faster moving crack may be greater.

Figure 6 (see p. 226) compares the transient ERRs for viscoelastic materials with different characteristic relaxation times, τ, with the transient ERR for an elastic

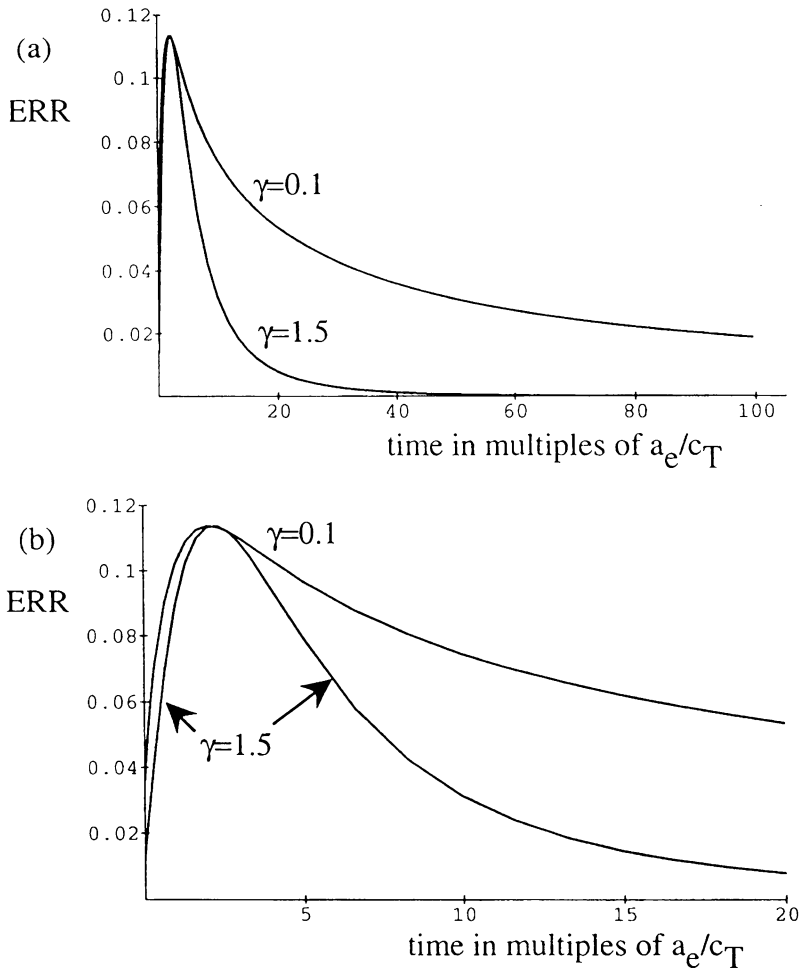

FIG. 5. Comparison of a scaled nondimensionalized ERR $G_K(t)/(L_e^2 a_e/(8\mu_\infty))$ such that the two speeds $\gamma = 0.1$ and $\gamma = 1.5$ have the same peak ERR. Both (a) and (b) show the same graph. Note in (a) the much faster convergence of $\gamma = 1.5$ to zero than $\gamma = 0.1$. In (b) it can be seen that the rise of each curve to its peak value is almost identical. $\alpha = 1$, $\tau = 1$, $\varepsilon = .01$, $a_e = 1$, and $k_1 = .25$ with wave speeds $c_R^* = .93$, $c_T^* = 1.00$, $c_L^* = 2.00$, $c_R = 3.09$, and $c_T = 3.32$.

material (the $\tau \to \infty$ limit) for the case of tractions that travel with the crack tip. It is seen that the longer the characteristic relaxation time τ, i.e., the more elastic-like the material, the faster the ERR converges to its steady-state value. Furthermore, this difference in convergence rate is greater for faster crack speeds. Figure 7 (see p. 227) shows a similar comparison of the ERRs for different relaxation times but for the case of applied traction that do not follow the crack tip. It is seen that the more elastic-like the material, the higher the peak ERR and the slower rate of decay of the ERR to zero. Again, this difference is enhanced by faster crack tip speeds.

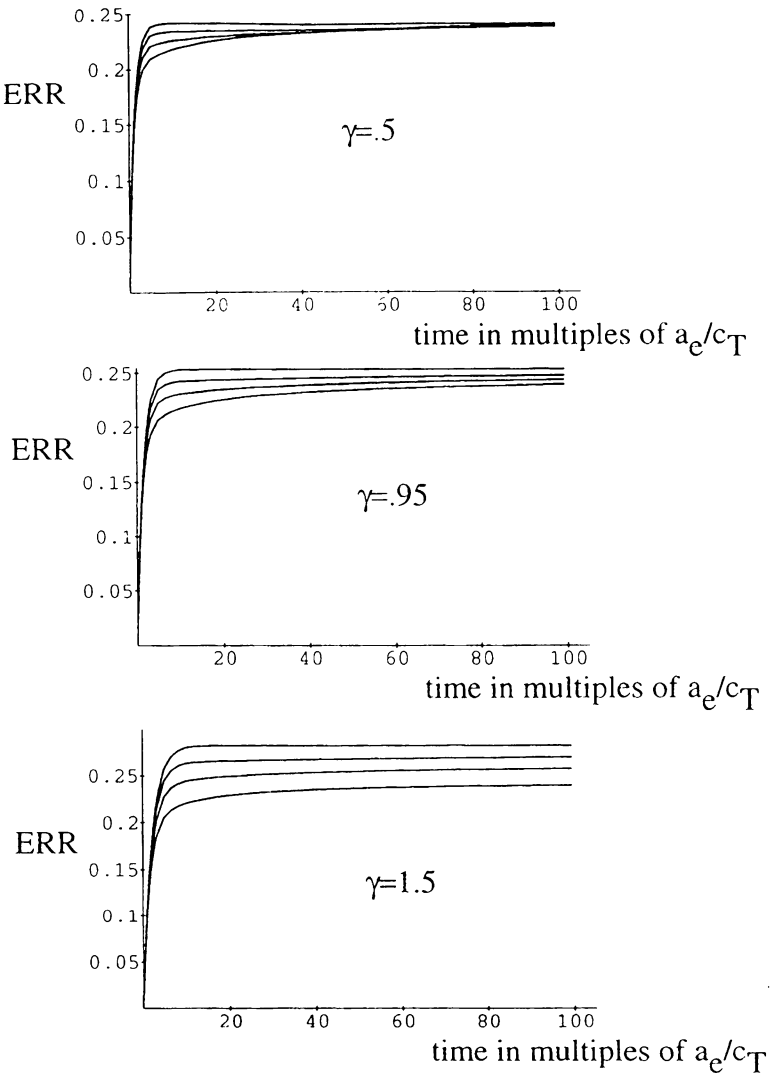

FIG. 6. A comparison of the nondimensionalized ERR, $G(t)/(L_e^2 a_e/(8\mu_\infty))$, for viscoelastic materials with different relaxation times τ at different crack speeds. The top curve is the ERR for an elastic material, $G_{el}(t)/(L_e^2 a_e/(8\mu_\infty))$ with the elastic shear modulus equal to the viscoelastic glassy shear modulus value. The second, third, and bottom curve in each graph correspond to $\tau = 5, 2, 1$ respectively. $\alpha = 1$, $a_e = 1$, $\varepsilon = .01$, and $k_1 = .25$ with wave speeds $c_R^* = .93$, $c_T^* = 1.00$, $c_L^* = 2.00$, $c_R = 3.09$, and $c_T = 3.32$.

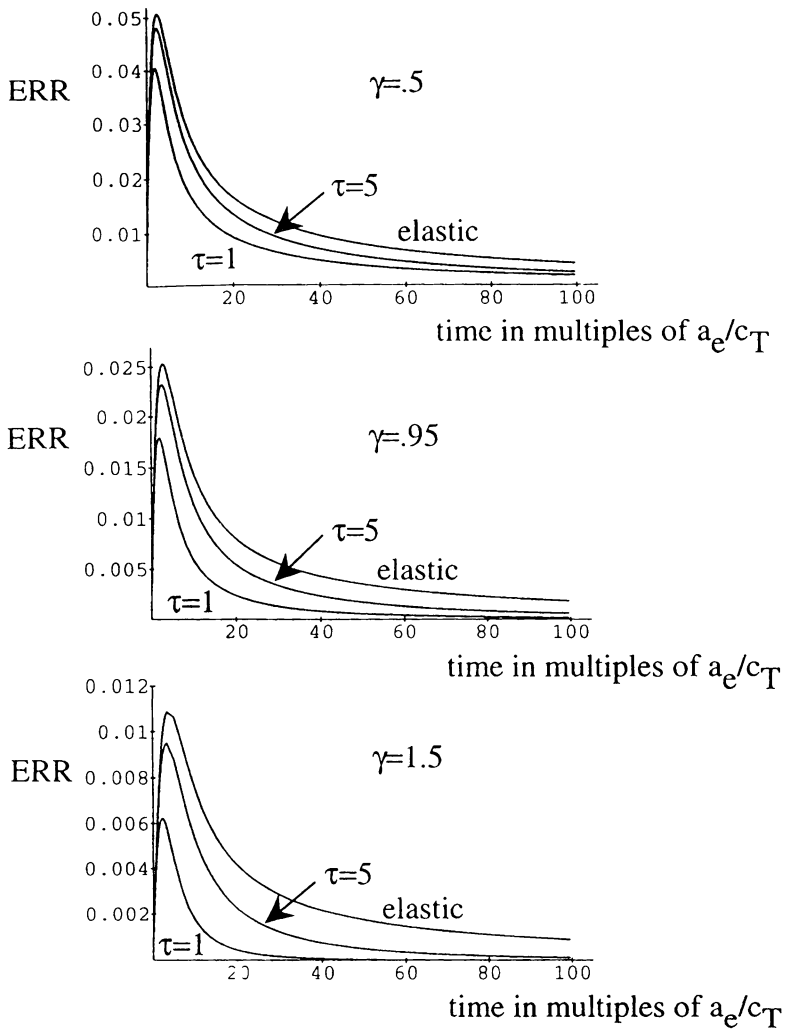

FIG. 7. A comparison of the nondimensionalized ERR, $G_K(t)/(L_e^2 a_e/(8\mu_\infty))$, for viscoelastic materials with different relaxation times τ at different crack speeds. The top curve is the ERR for an elastic material, $G_{K\,\mathrm{el}}(t)/(L_e^2 a_e/(8\mu_\infty))$ with the elastic shear modulus equal to the viscoelastic glassy shear modulus value. $\alpha = 1$, $a_e = 1$, $\varepsilon = .01$, and $k_1 = .25$ with wave speeds $c_R^* = .93$, $c_T^* = 1.00$, $c_L^* = 2.00$, $c_R = 3.09$, and $c_T = 3.32$.

REFERENCES

[1] J. D. Achenbach and A. Neimitz, *Fast fracture and crack arrest according to the Dugdale model*, Engrs. Fracture Mech. **14**, 385–395 (1981)

[2] D. D. Ang, J. Lund, and F. Stenger, *Complex variable and regularization methods of inversion of the Laplace transform*, preprint

[3] C. Atkinson, *A note on some dynamic crack problems in linear viscoelasticity*, Arch. Mech. (Arch. Mech. Stos.) **31**, 829–849 (1979)

[4] C. Atkinson and C. J. Coleman, *On some steady-state moving boundary problems in the linear theory of viscoelasticity*, J. Inst. Math. Appl. **20**, 85–106 (1977)

[5] C. Atkinson and J. R. D. List, *A moving crack problem in a viscoelastic solid*, Internat. J. Engrg. Sci. **10**, 309–322 (1972)

[6] C. Atkinson and C. Popelar, *Antiplane dynamic crack propagation in a viscoelastic strip*, J. Mech. Phys. Solids **27**, 431–439 (1979)

[7] B. Davies and B. Martin, *Numerical inversion of the Laplace transform: A survey and comparison of methods*, J. Comput. Phys. **33**, 2–31 (1979)

[8] E. B. Glennie and J. R. Willis, *An examination of the effects of some idealized models of fracture on accelerating cracks*, J. Mech. Phys. Solids **19**, 11–30 (1971)

[9] J. M. Herrmann and L. Schovanec, *Quasi-static mode* III *fracture in a nonhomogeneous viscoelastic body*, Acta Mech. **85**, 235–249 (1990)

[10] J. M. Herrmann and J. R. Walton, *On the energy release rate for dynamic transient anti-plane shear crack propagation in a general linear viscoelastic body*, J. Mech. Phys. Solids. **37**, 619–645 (1989)

[11] J. M. Hermann and J. R. Walton, *A comparison on the dynamic transient anti-plane shear crack energy release rate for standard linear solid and power-law type viscoelastic materials*, ASME J. Engrg. Res. Tech. **113**, 222–229 (1991)

[12] C. Popelar and C. Atkinson, *Dynamic crack propagation in a viscoelastic strip*, J. Mech. Phys. Solids **28**, 79–93 (1980)

[13] K. Ravi-Chandar and W. G. Knauss, *Dynamic crack-tip stresses under stress wave loading—a comparison of theory and experiment*, Internat. J. Fracture **20**, 209–222 (1982)

[14] K. Ravi-Chandar and W. G. Knauss, *An experimental investigation into dynamic fracture*: I. *Crack initiation and arrest*, Internat. J. Fracture **25**, 247–262 (1984)

[15] K. Ravi-Chandar and W. G. Knauss, *An experimental investigation into dynamic fracture*: II. *Microstructural aspects*, Internat. J. Fracture **26**, 65–80 (1984)

[16] K. Ravi-Chandar and W. G. Knauss, *An experimental investigation into dynamic fracture*: III. *On steady-state crack propagation and crack branching*, Internat. J. Fracture **26**, 141–154 (1984)

[17] L. Schovanec and J. R. Walton, *The energy release rate for a quasi-static mode* I *crack in a nonhomogeneous linearly viscoelastic body*, Engrg. Fracture Mech. **28**, 445–454 (1987)

[18] L. Schovanec and J. R. Walton, *The quasi-static propagation of a plane strain crack in a power-law inhomogeneous linearly viscoelastic body*, Acta Mech. **67**, 61–77 (1987)

[19] L. Schovanec and J. R. Walton, *The energy release rate for two parallel steadily propagating mode* III *cracks in a viscoelastic body*, Internat. J. Fracture **41**, 133–155 (1989)

[20] J. R. Walton, *On the steady-state propagation of an anti-plane shear crack in an infinite general linearly viscoelastic body*, Quart. Appl. Math. **39**, 37–52 (1982)

[21] J. R. Walton, *Dynamic steady-state fracture propagation in general linear viscoelastic material*, in Workshop on Dynamic Fracture (W. G. Knauss, K. Ravi-Chandar, and A. J. Rosakis, eds.), pp. 197–204, California Inst. of Tech., Pasadena, CA, 1983

[22] J. R. Walton, *The dynamic steady-state propagation of an anti-plane shear crack in a general linearly viscoelastic layer*, J. Appl. Mech. **52**, 853–856 (1985)

[23] J. R. Walton, *The dynamic energy release rate for a steadily propagating anti-plane shear crack in a linearly viscoelastic body*, J. Appl. Mech. **54**, 635–641 (1987)

[24] J. R. Walton, *The dynamic energy release rate for a steadily propagating mode* I *crack in an infinite, linearly viscoelastic body*, J. Appl. Mech. **112**, 343–353 (1990)

[25] W. T. Weeks, *Numerical inversion of Laplace transforms using Laguerre functions*, J. Assoc. Comput. Mach. 419–429 (1966)

[26] J. R. Willis, *Crack propagation in viscoelastic media*, J. Mech. Phys. Solids **15**, 229–240 (1967)